SEMI-ANNUAL TECHNICAL REPORT NO. 1

NEW TECHNIQUES FOR THE SYNTHESIS OF METALS AND ALLOYS

R. F. Bunshah

THE PROPERTIES OF RARE EARTH METALS AND ALLOYS

D. L. Douglass

UCLA-ENG-7112

March 1971

UCLA-ENG-7112
March 1971

SEMI-ANNUAL TECHNICAL REPORT NO. 1

I. New Techniques for the Synthesis of Metals and Alloys
(Principal Investigator - Professor R. F. Bunshah)
Office Phone: (213) 825-2210 or 825-5473

II. The Properties of Rare Earth Metals and Alloys
(Principal Investigator - Professor D. L. Douglass
Office Phone: (213) 825-1622 or 825-5534

Sponsor: The Advanced Research Projects Agency

Grant No.: DAHC 15-70 g 15

ARPA Order No.: AO 1643

Effective Date: July 1, 1970

Contract Expiration Date: June 30, 1972

Amount of Contract: $298,398

Classification: Unclassified

Materials Department
School of Engineering and Applied Science
University of California
Los Angeles, California

TABLE OF CONTENTS

Abstract

Two major areas of effort are encompassed:

I. New Techniques for the Synthesis of Metals and Alloys

The High Rate Physical Vapor Deposition (HRPVD) process is to be used for the following:

1. Preparation and characterization of Ni and Ni-20Cr alloy sheet
2. Synthesis of compounds Y_2O_3, TiC, Si_3N_4 by reactive evaporation and their characterization
3. Dispersion strengthened alloys, Ni-20Cr-Y_2O_3, Ni-20Cr-TiC and Ti-Y_2O_3

This report describes the HRPVD apparatus. Models for calculation of temperature and thickness distribution of the deposit are given.

II. The Properties of Rare Earth Metals and Alloys

Small amounts of certain rare-earth elements in Nickel-base alloys are known to markedly reduce the rate of oxidation at high temperatures and confer mechanical stability on the scales found. This program is directed at obtaining an understanding of the mechanisms and to characterize the oxidation behavior of Ni-20Cr containing Gd, La and Y and alloys based on composition Ni_3Al.

I. Introduction

This report describes research activities on ARPA Grant No. A 01643. The scope of the work is divided into two major areas of effort and further subdivided into four tasks as shown below.

1. New Techniques for the Synthesis of Metals and Alloys - Tasks I, II, and III. (Professor R. F. Bunshah - Principal Investigator)
2. The Properties of Rare Earth Metals and Alloys - Task IV. (Professor D. L. Douglass - Principal Investigator)

In the following each of the two areas and tasks will be described separately with the progress to date.

II. New Techniques for the Synthesis of Metals and Alloys - (Tasks I, II and III)

A. Background

High Rate Physical Vapor Deposition (HRPVD) Techniques[1,2,3,4,5,6,7,8] are to be used to prepare metallic alloys, ceramics, and metal-ceramic mixtures (dispersion strengthened alloys). The method consists of evaporation of metals, alloys and ceramics contained in water cooled crucibles using high power electron beams. The process is carried out in a high vacuum environment. The use of high power electron beams makes it possible to produce very high evaporation rates. The vapors are collected on heated metallic substrates to produce full density deposits at high deposition rates.

There are three (3) tasks in this section:

Task I: The preparation and characterization of Nickel and Ni-20Cr alloy sheet by the high rate physical vapor deposition process.

Task II: Synthesis and characterization of compounds by Reactive Evaporation. The compounds to be prepared are Y_2O_3, TiC and Si_3N_4.

Task III: Dispersion strengthened alloys produced by HRPVD Process, and their characterization. The specific alloys to be studied are:

1. Ni-20Cr-Y_2O_3 2. Ni-20Cr-TiC 3. Ti-Y_2O_3

Single source and two source evaporation methods will be used to produce these alloys.

The HRPVD process has several attractive features:

1. Simple, full density shapes (sheet, foil, tubing) can be produced at high deposition rates, $\geq$ 0.001" per minute thickness increment thus making it an economically viable process.

2. Metals and alloys of high purity can be produced.

3. Very fine grain sizes (1μ grain dia. or smaller) can be produced by controlling substrate temperature. Grain size refinement is produced by lowering the condensation temperature.

4. An alloy deposit may be produced from a single rod fed source. This occurs because the molten pool at the top of the rod is only 1/4" deep. The vapor composition is the same as that of the solid rod being fed into the molten pool. At equilibrium, the composition of the molten pool differs from that of the vapor or the solid feed. It is richer in those components having a low vapor pressure. The composition of the vapor is the product of the vapor pressure times the mol fraction of the component. For example, a Ti-6Al-4V alloy deposit where the differences in vapor pressure of Al and V are a factor of 5,000 at 1600°C can be produced by evaporation from a single source. The feed-rod is Ti-6Al-4V and the molten pool is much richer in V than in Al.

5. Two or more sources can be used to simultaneously deposit on the same substrate thus conferring the ability to produce complex alloys. For example, an alloy with a 2 or 3 component solid solution matrix may be evaporated from one source and another metal or ceramic for the dispersed phase from another source. The dispersion size and spacing should be very fine since the deposition is occurring from the vapor phase.

The unique feature of this process is that all of the above benefits can be obtained <u>simultaneously</u>.

It should be noted that the condensation temperature is a very important process variable. Bunshah and Juntz[8] found that for titanium, as the deposition temperature is lowered the grain size of the fully dense deposit becomes finer. At very low temperatures (~25% of the melting point) the deposit has less than full density. Since a fine grain sized microstructure represents an optimum condition of strength and toughness in a material, the importance of control of the deposition temperature becomes obvious.

B. Scope of Work

The main tasks on this contract are the preparation and testing of the various alloys, ceramics and dispersion strengthened alloys as outlined in Section I above. Very essential to the preparation of suitable test specimens are two other factors:

1. Design of the apparatus for high rate physical vapor deposition.
2. Theoretical calculation of the thickness distribution and temperature distribution of the deposited material which in this case is in the form of a sheet.

Both of these tasks are essential preliminaries to the main scope of work and are detailed below.

C. High Rate Physical Vapor Deposition Apparatus for Alloys, Dispersion Strengthened Alloys and Ceramics

Such an apparatus is quite complex and has many state-of-the-art features. The design requirements for such an apparatus are as follows:

1. High rate evaporation of metals, alloys or ceramics from one source or two sources simultaneously. Sources should be rod-fed to permit long time uniform evaporations.
2. Electron beam heating incorporated into the sources to get high evaporation rates. In addition, beam scanning of the source should be available in one of the sources which is used for the direct evaporation of ceramics or dielectrics.

3. Substrate holder capable of:

   a) Heating the substrate to an elevated temperature and controlling it at the desired temperature. This is necessary to produce a fully dense deposit. The apparatus will have capability of:-

      i. heating a 10" x 10" substrate up to 1000°C by radiant heating from the back.

      ii. direct resistance heating of one or more 1/2" x 3" strips to 1500°C.

   b) Rotation of the 10" x 10" substrate and the ability to tilt the axis of rotation up to 45° from the vertical. This is necessary to produce a uniform thickness of deposit over the entire substrate.

4. A high vacuum environment capable of maintaining a working pressure of 5.10^{-6} torr or lower and a base pressure of 2.10^{-7} torr or lower. The vacuum environment should be monitored using residual gas analyzers. The best vacuum techniques should be used to keep contamination of the deposit from back-streaming and other sources to a minimum.

5. A liquid pool level monitor to keep the height of the liquid pool at the desired level. This is necessary to keep the alloy composition in the vapor phase at a constant value.

6. Capability to bleed gases or gas mixtures at the desired partial pressures in the vicinity of the substrates. This is necessary to carry out reactive evaporation processes effectively.

7. The ability to feed raw material and melt it into evaporant stock. This feature is very desirable as the raw material for evaporant stock should have very low gas content to avoid spattering of liquid droplets during evaporation. Not all evaporant materials can be purchased in the desired form. Rod fed electron beam sources also require the feed rod to have outside diameter to fit the inside diameter of the opening in the source after allowing for thermal expansion. Evaporant materials may not be available in the desired rod sizes.

8. The ability to measure the temperature of the molten pool preferably with an optical or total radiation pyrometer. This requires clear visual access to the molten pool and the ability to keep the window free of deposited vapors. The latter devices are commercially available.

D. Temperature Distribution and Thickness Distribution of the Deposit

Consider a flat substrate located at some distance from an evaporation source. For a point source or a small flat plate source the vapor density will decrease proportional to cos θ, where θ is the angle between the vertical axis of the source and the location on the substrate (Cosine distribution law). Thus the deposit will be tapered from the center to the edge. This is not too desirable as it will affect the specimen yield (i.e., the number of specimens that can be machined from a deposit without grinding it to uniform thickness) as well as the temperature distribution from the center to the edge of the specimen. The percent thickness variation from center to edge on a deposit varies with the distance between source and substrate and usually becomes less than 10% at source-substrate distance of 10 times the source diameter. In electron beam heated sources the thickness variation is somewhat greater than that produced by other sources and also depends on the particular material being evaporated. The total thickness per unit time also varies inversely as the square of the source-substrate distance. Therefore a calculated estimate of the deposit thickness and thickness variation as a function of source-substrate distance is necessary for proper planning of the experiment. One method of producing uniform thickness deposits is to collect them on rotating substrates with the rotation axis inclined about 30° to the horizontal plane. For electron beam sources, the exact angle would have to be determined by experimentation.

The deposition temperature is very important. At very low deposition temperatures the deposit will not be fully dense. At higher deposition temperatures, the deposit will be fully dense. The grain size of the deposit will coarsen as the deposition temperature gets higher. Since the strength and toughness of a deposit decrease with increasing grain size,

the selection of the deposition temperature becomes a very important process variable. It should be high enough to produce a fully dense deposit and yet not too high to permit grain size coarsening.

An estimation of the temperature of a deposit produced by high rate physical vapor deposition processes is somewhat complicated. A new method has been developed for making such a calculation. By performing an energy balance between energy gain and energy loss of the deposit. The deposit receives energy from three sources -

1. Radiation from the hot source.
2. Latent heat of condensation of the vapor and cooling of the deposit to the deposition temperature.
3. Heat of reaction when a deposit species reacts with the gas phase to form a compound. This is applicable in the case of reactive evaporation only.

In a vacuum environment where the substrate is supported so as to minimize conductive heat transfer to the holder, the principal mode of heat loss is radiative. Radiative heat loss occurs from the deposit face as well as the back side of the substrate. In addition, there is a small energy loss necessary to heat the substrate to the experimental temperature; however this factor is small for these substrates and is zero once equilibrium has been established. The time to attain equilibrium is usually less than a minute and in most cases a very small fraction of the total deposition time.

The experimental variables are:

1. Nature of evaporating species (metal, alloy, compound) and the vapor pressure of the component species.
2. Temperature of the source and evaporation rate.
3. Source diameter.
4. Source-substrate distance.
5. Substrate material.
6. Substrate material thickness.

7. Thermodynamic properties of condensate (latent heat of condensation, specific heat, vapor pressure).
8. Heat of reaction in the case of reactive evaporation.
9. The total hemispherical emittance of the evaporant as a function of evaporation temperature.
10. The total hemispherical emittance of the deposit as a function of condensation temperature.
11. The total hemispherical emittance of the substrate as a function of condensation temperature.
12. The absorptance of the deposit as a function of condensation temperature.

With a large number of variables, it is essential to make a computational estimate of the temperature distribution of the deposit to minimize the number of experiments performed. A computer program has been written to make such an estimate.

These factors are considered in detail in Supplements 1 and 2 attached to this report. These Supplements are self-contained documents dealing with the following topics:

1. Model for calculating the deposit temperature in high rate physical vapor deposition processes.
2. Temperature and Thickness Distribution on the Substrate During High Rate Physical Vapor Deposition of Materials.

They are to be submitted for publication.

E. Progress to date (July 1, 1970 - January 31, 1971)

1. High Rate Physical Vapor Deposition Process Apparatus.

The design of this apparatus was completed, specifications written, quotations obtained, and order placed. The apparatus will be delivered in February 1971.

2. Theoretical Calculation of the Temperature and Thickness Distribution of the Deposit.

A new method has been developed to calculate the thickness and temperature distribution of the deposit. The importance of this has been explained above. Supplements 1 and 2 attached to this report describe this work in detail. Temperature and thickness variation for yttrium and yttria (Y_2O_3)

deposits have been used to illustrate the calculations. Y_2O_3 is produced by reactive evaporation between metal vapors and oxygen introduced into the gas phase. The range of variables to be explored experimentally is defined from the calculations for the deposition of Y and Y_2O_3. They are:

1. Temperature of the source - 2300 to 2600°K.
2. Source to substrate distance - 25 to 35 cm.
3. Diameter of source - 1.0" to 1.5".
4. Substrate material - buffed stainless steel and copper.
5. Substrate thickness - .001 to .005".
6. Substrate size (diameter) - 8 to 20 cm.

3. Deposition of Ni-20Cr alloy.

Using a single-source apparatus available at UCLA, fully dense ductile deposits of Ni-20Cr alloy have been made with good success.

F. Future Work

In the next half year period, the following work is scoped:

1. Installation and operation of the 2 source vacuum evaporation apparatus.

2. Calculations of temperature and thickness distribution of the deposit for TiC, Si_3N_4, Ni and Ni-20Cr will be carried out.

3. Development of a model relating the composition of the vapor phase in an alloy deposit to the composition of the molten pool. This model will be developed for rod-fed electron-beam heated sources. The variables to be considered are temperature of the molten pool, volume of the molten pool, and time to attain equilibrium composition of the pool.

4. Feasibility studies on the production of Y_2O_3, TiC and Si_3N_4 by reactive evaporation.

5. Deposition of Ni and Ni-20Cr alloy sheets and study of their structure and properties.

G. Personnel

The following personnel have been working on the project:
Principal Investigator - Professor R. F. Bunshah (since July 1, 1970)
Graduate Students - Raymond Chow and R. Nimmagadda (since July 1, 1970)
Post Doctoral Fellow - Dr. A. C. Raghuram (as of February 1, 1971)
Technician - Mr. Harold Willey (since November 1, 1970)

III. The Properties of Rare Earth Metals and Alloys - (Task IV)

A. Introduction

The presence of small amounts of certain rare earth elements in nickel-base alloys is known to markedly reduce the rate of oxidation at high temperatures and to exert a highly beneficial effect on the mechanical stability of the scales formed. The effect is disproportionate to the amount added. Generally, a fraction of a percent, e.g., approximately 0.1 to 0.3%, is sufficient. In particular, the resistance to exfoliation of the scales becomes outstanding.

The mechanism by which these effects occur is not known and has been subject to rather wild speculation. The program in progress is directed at obtaining an understanding of the mechanism and to characterize the oxidation behavior of certain alloys containing rare earth additions.

B. Experimental Work

1. Alloy Preparation

Melting and fabrication of alloys was subcontracted to Stanford Research Institute. Charges of about 400 gms. total were triple arc-melted in argon with an inert electrode on a water-cooled copper hearth. The buttons were flipped over after each melting and remelted a total of three times. It is noteworthy that the alloys based on the composition Ni_3Al

(approximately 13 w/o Al) all cracked upon cooling of the arc-melted buttons. These alloys were found to be extremely brittle and could not be successfully melted, much less subsequently fabricated, in spite of numerous attempts.

The other base material was Ni-20Cr to which was added Gd, La, and Y, initially in the amount of 1 w/o and subsequently in the amount of 0.5 w/o. These compositions produced sound buttons which were amenable to subsequent fabrication.

The buttons of the Ni-20Cr base alloys were hot rolled to 0.030" thick sheet at temperatures in the range of 1200 to 1300°C. The surface oxide was removed by sandblasting, and the sheet was cold-rolled to 0.020" in thickness.

Oxidation samples were sheared from the cold-rolled sheet, cleaned, and annealed for 20 minutes at 900°C. They were weighed and then subjected to oxidation tests.

2. Oxidation Tests

Thermal gravimetric analysis was performed in a Harrop Unit that required about 40 minutes to reach a temperature of 1200°C. The weight gain increased rapidly with time during heat up commencing at a temperature of about 500°C. Although the system could be evacuated readily, it was not feasible to heat in vacuum and then introduce the oxidizing environment. This problem results from the difficulty of establishing the null point in the system which employs a linear differential transformer to record movement (and hence weight change) of the balance arm.

The rapid increase of weight at low temperatures is most likely due to the initial formation of NiO, the formation of this oxide at low temperatures being much more rapid than the formation of other oxides, e.g., Cr_2O_3, $NiCr_2O_4$, or a rare earth oxide. This behavior does not occur at 1200°C.

In order to circumvent the above-mentioned problem, the sample was introduced quickly into another furnace at the same temperature and held for one hour. This permitted the oxides to form which are characteristically formed at the temperature of interest. The sample was removed, reweighed, and placed in the TGA unit. It was then possible to calibrate the unit and then heat up with virtually no change in weight taking place during the heating period. The time at which the desired temperature was reached was then taken as 60 minutes, and the test was carried out for the desired time period.

3. Results

Kinetics curves have been obtained for Ni-20Cr and for Ni-20Cr-1Gd using the technique described. Runs were made at 1200°C in air. The alloy containing Gd showed a very rapid initial increase in weight followed by a continuously decreasing rate (less than parabolic). The presence of Gd resulted in a decreased rate compared to plain Ni-20Cr.

C. Personnel

The following personnel have been working on Part II of this program:

Principal Investigator - Professor D. L. Douglass

Graduate Student - J. R. Kuenzly

References

1. Bunshah, R. F., "Superpurification of Metals by Vacuum Distillation: A Theoretical Study," Trans. Vac. Met. Conf., 1963, AVS, 121.

2. Bunshah, R. F., and Juntz, R. S., "Purification of Beryllium by Crucible Free Melting and Distillation Process" in Beryllium Technology, Gordon and Breach, 1964, 1.

3. Bunshah, R. F., "Impurity Removal by Distillation of Beryllium from the Solid State," Proceedings, Int'l. Conf. on Beryllium, Grenoble, France, 1965, Presses Universitaries de France, 108 Blvd. St. Germain, Paris, 6, 63.

4. Bunshah, R. F., and Juntz, R. S., "The Purification of Beryllium by Vacuum Melting followed by Vacuum Distillation in an Electron Beam Furnace with Simultaneous deposition of Sheet," Trans. Vac. Met. Conf., 1966, AVS, 209.

5. Bunshah, R. F., "The Effect of Purification on Some Mechanical Properties of Beryllium," Metals Engineering Quarterly, Nov. 1964, 8.

6. Bunshah, R. F., and Juntz, R. S., "Electron Beam Distillation Furnace for Reactive Metals: Design Considerations and Operating Experience," Trans. Vac. Met. Conf., 1965, AVS, 200.

7. Bunshah, R. F. and Juntz, R. S., "Design Considerations for the Production of Massive Deposits of Alloys by Evaporation from Multiple Electron Beam Heated Sources," Trans. Vac. Met. Conf., 1967, AVS, 799.

8. Bunshah, R. F., and Juntz, R. S., "Influence of Condensation Temperature on Microstructure and Mechanical Properties of Titanium Sheet," to be published.

SUPPLEMENT-1

Model for Calculating the Deposit Temperature in High Rate Physical Vapor Deposition Process

Objective

The high rate physical vapor deposition process is used to produce metals or alloys of high purity, full density, small grain-size and controlled thickness. The substrate temperature during deposition is the most important experimental parameter for controlling the grain-size and density of the deposit. As grain-size decreases, the strength and toughness of the material increase. Therefore, it is important to develop a model for calculating the temperature distribution of the deposit. In this paper, we will postulate a model for calculating the temperature of the deposit and then proceed to verify the model by calculating the deposit temperature for experimental conditions given in the literature for the evaporation of titanium[1] and comparing the calculated temperature to the measured temperature.[1] The temperatures of the deposit and the substrate on which it is deposited are the same since they are in intimate thermal contact. This has been experimentally verified by Bunshah and Juntz.[1]

Equation of Energy Balance

The experimental set-up for high rate physical vapor deposition processes (HRPVD) is shown in Fig. 1. The metal is contained in a water-cooled copper crucible and heated by an electron beam source. The metal vapors are condensed on a metallic substrate located above the source.

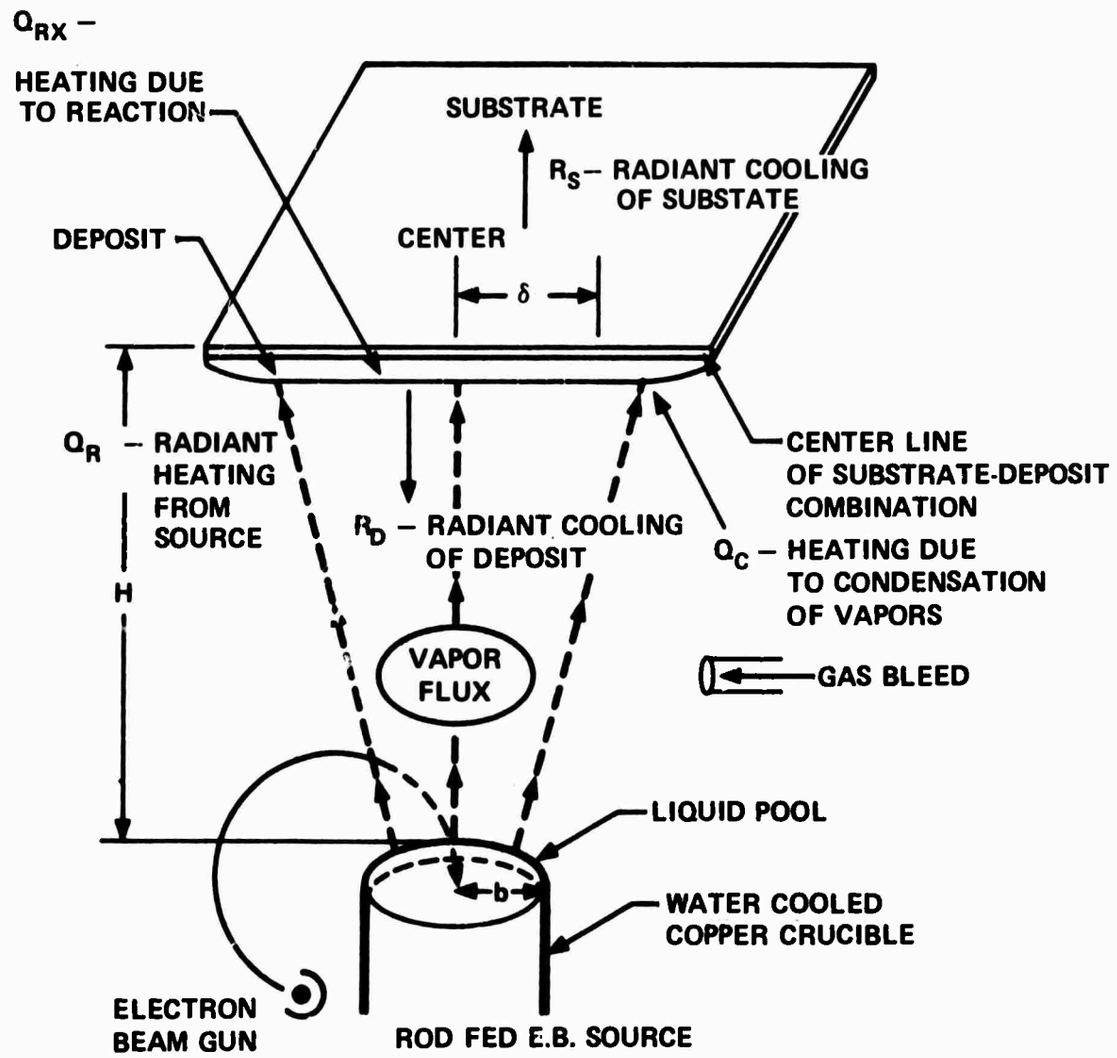

Figure 1. Schematic of High Rate Physical Vapor Process

The model for calculation of the deposit temperature is based on the energy balance between the energy input and output of the substrate. The energy input to the substrate consists of three terms:

- Q_R - the radiant energy from the source at Temperature T_1
- Q_C - energy supplied by the condensation of metal vapors
- Q_{Rx} - the heat of reaction for reactive evaporation i.e., if a reaction occurs between the condensing vapors and a gas phase on the substrate or between two metal vapors condensing on the substrate. For simple condensation of metal or alloy vapors this term is zero.

The energy output from the substrate consists of the following terms:

- R_d - energy radiated from the deposit side at temperature T_2 of the substrate
- R_s - energy radiated from the back side of the substrate at temperature T_2 i.e., the side away from the source
- H_s - energy necessary to heat the substrate material to the substrate temperature T_2
- H_d - energy necessary to heat the material already deposited if at a lower temperature, to the substrate temperature T_2

We can now write the equation of energy balance as:

$$Q_R + Q_C + Q_{Rx} = R_d + R_s + H_s + H_d \qquad (1)$$

Initially during the process, the energy input will exceed the heat output and the temperature of the substrate-deposit combination will rise, thus causing an increased energy loss from the substrate. Since the energy input to the substrate deposit combination is constant and the output is proportional to T_2^4 (T_2 being the substrate temperature), a steady state will be reached. Under steady state conditions, H_s and H_d in equation 1 are zero and the equation of energy balance becomes

$$Q_R + R_c + Q_{Rx} = R_d + R_s \qquad (2)$$

We are also assuming here that the rate of heat loss by conduction of the substrate and deposit to adjoining areas is so small in comparison

to the other energy loss terms that it can be neglected as shown in Appendix 1.

Let us now examine each term in equation 2 in detail.

Q_R - energy absorbed by the substrate at temperature T_2 from the source at temperature T_1

$$Q_R = \int_0^\infty \varepsilon_1(\lambda,T_1)\, \alpha_s(\lambda,T_2)\, W(\lambda,T_1)\, A_1\, F_{A_1 - dA_2}\, t\, d\lambda \qquad (3)$$

where $\varepsilon_1(\lambda,T_1)$ = spectral emittance of source at temperature T_1

$\alpha_s(\lambda,T_2)$ = spectral absorptance at substrate temperature T_2

$W(\lambda,T_1)$ = Planckian radiant emittance at temperature T_1

$$= \frac{c_1}{\lambda^5} \frac{1}{\exp(c_2/T_1) - 1}$$

c_1 = $2\pi hC^2 = 3.7413 \pm 0.003 \times 10^{-12}$ watt cm^2

c_2 = $\frac{hc}{k} = 1.43884 \pm 0.0008$ cm degree

h = Planck's constant

k = Wave number

λ = Wave length

A_1 = Area of the source

dA_2 = Infinitesimal area at the center of deposit

$F_{A_1 - dA_2}$ = Configuration factor for radiation traveling from A_1 to dA_2

t = duration of experiment

If we apply the reciprocity rule for the configuration factor[2],

$$A_1\, F_{A_1 - dA_2} = dA_2\, F_{dA_2 - A_1} \qquad (4)$$

where $F_{dA_2 - A_1}$ is the configuration factor for radiation travelling from dA_2 to A_1.

$$\therefore Q_R = dA_2 \; F_{dA_2 - A_2} \; t \int_0^\infty \varepsilon_1(\lambda,T_1)\alpha_s(\lambda,T_2)W(\lambda,T_1)\, d\lambda \qquad (5)$$

R_d - energy radiated by the infinitesimal area dA_2 of the deposited material

$$R_d = dA_2 \; t \int_0^\infty \varepsilon_d(\lambda,T_2)\, W(\lambda,T_2)\, d\lambda \qquad (6)$$

where $\varepsilon_d(\lambda,T_2)$ = spectral emittance of the deposit at substrate temperature T_2

$W(\lambda,T_2)$ = Planckian radiant emittance at temperature T_2.

R - energy radiated by the infinitesimal area of the substrate dA_2

$$R_s = dA_2 \; t \int_0^\infty \varepsilon_s(\lambda,T_2)\, W(\lambda,T_2)\, d\lambda \qquad (7)$$

where $\varepsilon_s(\lambda,T_2)$ = spectral emittance of the substrate at substrate temperature T_2

Q_c - energy supplied by the latent heat of condensation of metal vapors

$$Q_c = H_s + H_\ell + H_t \qquad (8)$$

where H_s = energy released on cooling of metal vapors from source temperature T_1 to the condensation temperature T_c plus energy released on cooling the deposited solid from T_c to substrate temperature T_2

H_ℓ = latent heat of condensation at temperature T_c

H_t = latent heat of phase transformation in the solid if applicable

Substituting equations 5, 6, 7, and 8 into the equation of energy balance (2) we get:

$$dA_2 \; F_{dA_2 - A_1} \; t \int^\infty \varepsilon_1(\lambda,T_1)\, \alpha_5(\lambda,T_2)\, W(\lambda,T_1)\, d\lambda + \Delta H_3 + \Delta H_\ell + \Delta H_t$$

$$= dA_2 \; t \int_0^\infty \varepsilon_d(\lambda,T_2)\, W(\lambda,T_2)\, d\lambda$$

$$+ dA_2 \; t \int_0^\infty \varepsilon_s(\lambda,T_2)\, W(\lambda,T_2)\, d\lambda \qquad (9)$$

Analysis for Calculation of Total Emittance $\varepsilon(T)$ and the Product of Total Emittance and Absorbtance $\varepsilon(T) \times \alpha(T)$ from Spectral Absorbtance $\alpha(\lambda,T)$ Data.

Equation (9) involves terms containing complicated integrals. We will now present an analysis to simplify this equation and enable us to calculate substrate temperature T_2.

This analysis contains two assumptions:

(1) Emittance of a metal is independent of the wave-length, the familiar grey-body assumption used in the derivation of Stefan-Boltzman Law of Radiation.

(2) The spectral absorbtance of the deposit $\varepsilon_d(\lambda,T)$ varies very slowly with substrate temperature, i.e., for the purposes and within the scope of this model it is essentially independent of temperature.

The validity of these assumptions will be tested by computation of the substrate temperature and comparison with experiment. Making the grey-body assumption, equation 6 which gives the energy radiated by an infinitesimal area of the deposit dA_2 becomes:

$$R_d = dA_2 \; t \int_0^\infty \varepsilon_d(\lambda,T_2)\, W(\lambda,T_2)\, d\lambda = \varepsilon_d(T_2)\, \sigma\, T_2^{\,4}\, dA_2\, t \qquad (10)$$

where σ = Stefan-Boltzmann Constant = 5.668×10^{-5} ergs/sec $cm^{2}{}^{\circ}K^4$

$\varepsilon_d(T_2)$ = Total hemispherical emittance of the deposit at substrate temperature T_2

Equation (10) can be written as

$$\varepsilon_d(T_2) = \frac{\int_0^\infty \varepsilon_d(\lambda,T_2) W(\lambda,T_2)\, d\lambda}{\sigma\, T_2^{\,4}}$$

$$= \int_0^1 \varepsilon_d(\lambda,T_2)\, df\,(\lambda,T_2) \qquad (11)$$

where

$$f(\lambda,T_2) = \frac{\int_{\lambda}^{\infty} \frac{c_1\, d\lambda}{\lambda^5\{\exp(c_2/\lambda T_2) - 1\}}}{\sigma\, T_2^{\,4}} \qquad (12)$$

The function $f(\lambda,T)$ has been defined in reference 3.

Since Kirchoff's law states the spectral emittance is equal to the spectral absorptance at the same temperature, equation 11 can be written as

$$\varepsilon_d(T_2) = \int_0^1 \alpha_d(\lambda,T_2)\ df\ (\lambda,T_2) \qquad (13)$$

Similarly,

$$_s(T_2) = \int_0^1 \alpha_s(\lambda,T_2)\ df\ (\lambda,T_2) \qquad (14)$$

where,

$\varepsilon_s(T_2)$ = total hemispherical emittance of the substrate at substrate temperature T_2.

$\alpha_s(\lambda,T_2)$ = spectral absorbtance of substrate at substrate temperature.

If we assume the variation of $\alpha_d(\lambda,T_2)$ and $\alpha_s(\lambda,T_2)$ with temperature are very small, i.e. they are temperature insensitive, equations 13 and 14 reduce to equations 15 and 16 respectively.

$$\varepsilon_d(T_2) = \int_0^1 \alpha_d(\lambda)\ df\ (\lambda,T_2) \qquad (15)$$

$$\varepsilon_s(T_2) = \int_0^1 \alpha_s(\lambda)\ df\ (\lambda,T_2) \qquad (16)$$

Similarly, by applying the grey-body assumption, Q_R, the energy absorbed by the deposit at temperature T_2 from source radiation at temperature T_1 is:

$$Q_R = \int_0^{\infty} \alpha_d(\lambda,T_2)\ \varepsilon_1(\lambda_1,T_1)\ W(\lambda,T_1)\ d\lambda\ dA_2\ t$$

$$= \alpha(T_2)\ \varepsilon(T_1)\ \sigma T_1^{\,4}\ dA_2\ t \qquad (17)$$

where $\alpha(T_2)$ = total hemispherical absorbtance of deposit at substrate temperature T_2

$\varepsilon(T_1)$ = total hemispherical emittance of source at source temperature T_1

Equation (17) can be written as -

$$\alpha(T_2)\ \varepsilon(T_1) = \frac{\int_0^\infty \alpha_d(\lambda,T_2)\ \varepsilon_1(\lambda,T_1)\ W(\lambda,T_1)d\lambda}{\sigma\ T_1^4} \tag{18}$$

Applying Kirchoff's law $\varepsilon_1(\lambda,T) = \alpha_1(\lambda,T)$ and equation 18 becomes

$$\alpha(T_2)\ \varepsilon(T_1) = \frac{\int_0^\infty \alpha_d(\lambda,T_2)\alpha_1(\lambda,T_1)\ W(\lambda,T_1)\ d\lambda}{\sigma\ T_1^4}$$

Again assuming that the spectral absorbtance is essentially insensitive to temperature, the above equation reduces to

$$\alpha(T_2)\ \varepsilon(T_1) = \frac{\int_0^\infty \alpha_d^2(\lambda)W(\lambda,T_1)\ d\lambda}{\sigma\ T_1^4}$$

$$= \int_0^1 \alpha_d{}^2(\lambda)\ df(\lambda,T_1) \tag{19}$$

where $\alpha_d(\lambda)$ = spectral absorbtance of deposit of source material whose value is temperature insensitive

and $f(\lambda,T_1)$ = the function defined in equation 12 above at temperature T_1.

Equations 15, 16, and 19 can be used to simplify the equation of energy balance (equation 9) which now becomes

$$dA_2\ F_{dA_2-A_1}\ t\ \sigma\ T_1^4 \int_0^1 \alpha_d{}^2(\lambda)\ df(\lambda,T_1)\,d\lambda + H_s + H_\ell + H_t$$

$$= dA_2\ t\ \sigma\ T_2^4 \int_0^1 \alpha_d(\lambda)\ df(\lambda,T_2) + dA_2\ t\ \sigma\ T_2^4 \int_0^1 \alpha_s(\lambda)\ df(\lambda,T_2) \tag{20}$$

Equation 20 is much easier to evaluate than equation 9 because the integrals in equation 20 can be evaluated using Simpson's Rule. We will illustrate this for the R_d term which is stated in equation 15 and is the first term on the right-hand side of equation 20.

The function $f(\lambda,T_2)$ in equation 12 can be expanded to

$$f(\lambda,T_2) = \frac{\int_{\lambda}^{\infty} \frac{2\pi hc^2}{\lambda^5} \frac{d\lambda}{\exp(hc/k\,T_2) - 1}}{\sigma\, T_2^{\,4}} \tag{21}$$

We note that the function $f(\lambda,T_2)$ is a function of λ and T_2. Its values have been tabulated by Edwards in reference 3. In addition, the data for the spectral absorbtance of Ti, $\alpha_d(\lambda)$ at room temperature are given in figure 2.[3] In the following Table I, we have tabulated these values and applying Simpson's Rule we get

$$\varepsilon_d(T_2) = \int_0^1 \alpha(\lambda)\, df = \frac{0.8 \times 2.76}{12} = 0.184$$

Similarly we can evaluate the other integrals in equation 20.

Comparison of Calculated Deposit Temperatures with Measured Values

We shall calculate the deposit temperature for the experimental conditions for Runs 40 and 41 in reference 1 as shown in Table II. For the experimental geometry used, $F_{dA_2-A_1}$, the configuration factor from an infinitesimal area on the substrate dA_2 to the source area A_1 is 0.0107. The thermodynamic and thermophysical values with symbols used are listed in Table III. We will illustrate the calculation for Run 40.

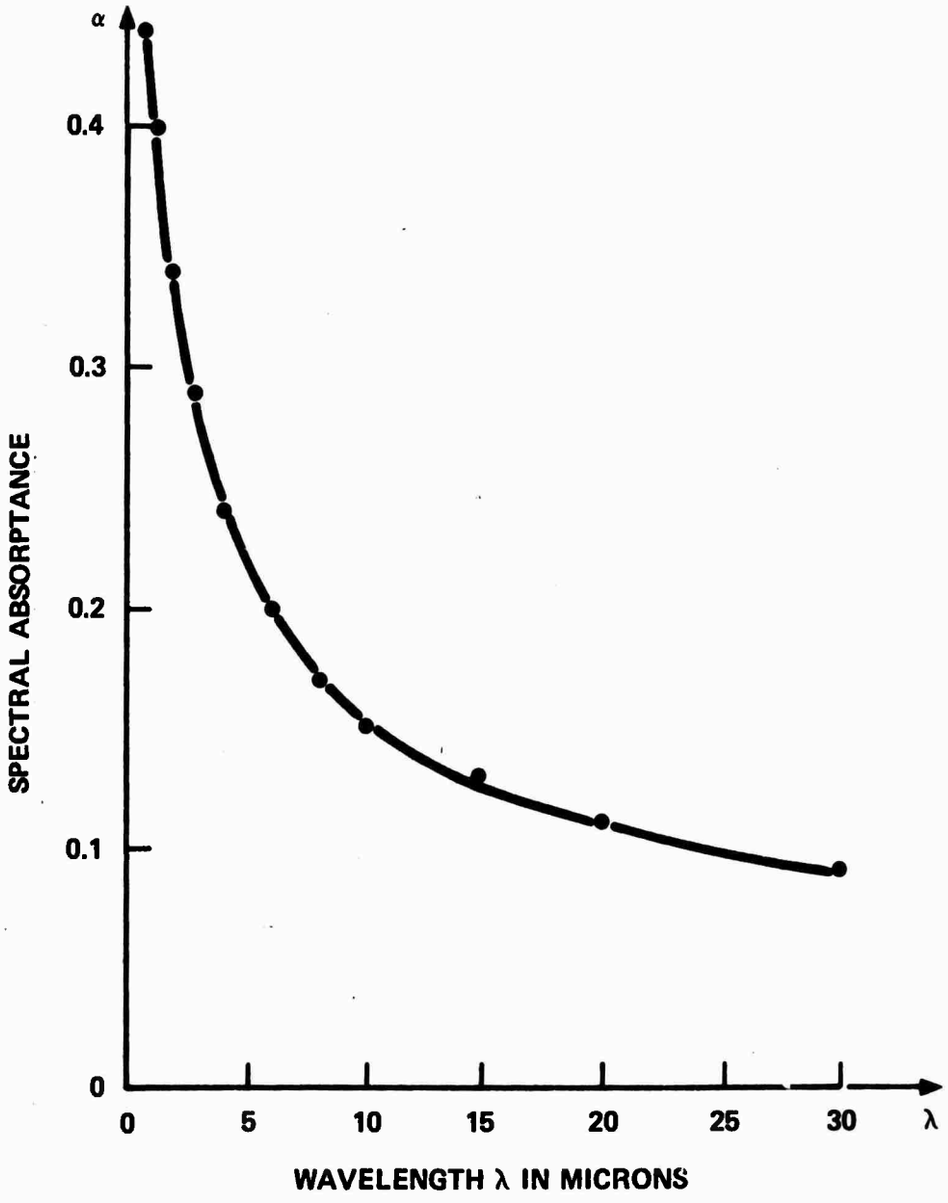

Figure 2. Spectral Absorptance of Titanium vs Wavelength

$$Q_R = dA_2 \, F_{dA_2-A_1} \, t \, \sigma \, t_1^4 \int_0 \alpha_d^2(\lambda) \, df(\lambda, T_1)$$

$$= dA_2 \times 0.0107 \times 3600 \times 5.67 \times 10^{-5} \times (2283)^4 \times 0.095$$

$$= 53.8 \times 10^8 \times dA_2 \text{ ergs} \qquad (23)$$

Q_c is evaluated by cooling the metal vapors from source temperature 2283°K to 1735°K, condensing them to solid at 1735°K and cooling the solid to the substrate temperature T_2. Now,

$$Q_c = H_s + H_\ell + H_t$$

$$H_s = \left[\int_{1735}^{2283} C_{p_1} \, dT + \int_{T_2}^{1735} C_{p_2} \, dT \right] \rho \, \delta \, dA_2 \qquad (24)$$

$$= [548 \times 5.1 + (1735 - T_2)] \times 10^6 \times 4.6 \times 0.094 \times dA_2 \text{ ergs}$$

where ρ = density = 4.6 g/cm^3 for Ti and δ = thickness of Ti deposit near center = 0.094 cm.

$$H_\ell \text{(at 7735°K)} = L \, \rho \, \delta dA_2 = 9.72 \times 10^{10} \times 4.6 \times 0.094 \times dA_2 \text{ ergs} \qquad (25)$$

H_t = energy associated with the latent heat of transformation of α to β at 1155°K

$$= 8.86 \times 10^8 \times 4.6 \times 0.094 \times dA_2 = 3.83 \times 10^8 \text{ ergs} \qquad (26)$$

$$R_d = dA_2 \; t \; \sigma \, T_2^4 \varepsilon_d(T_2)$$

$$= dA_2 \times 3600 \times 5.67 \times 10^{-5} \times T_2^4 \times 0.184$$

$$= 3.76 \times 10^{-2} \times T_2^4 \times dA_2 \text{ ergs} \qquad (27)$$

$$R_s = dA_2 \, t \, \sigma \, T_2^4 \, \varepsilon_s(T_2)$$

Substituting the value of $\varepsilon_s(T_2)$ for stainless steel as 0.22

$$R_s = dA_2 \times 3600 \times 5.67 \times 10^{-5} \times T_2^4 \times 0.22$$

$$= 4.49 \times 10^{-2} \times T_2^4 \times dA_2 \text{ ergs} \qquad (28)$$

Substituting equations 23, 24, 25, 26, 27, 28 into equation 20 we get a biquadratic equation containing a T_2^4 and T_2 term.

Solving for T_2 we get T_2 = 895 °K for Run 40

Similarly we calculate T_2 = 913 °K for Run 41.

Table IV compares the calculated the experimental values of the deposit temperatures and the percent difference in values. The agreement is excellent, the difference being only 2°K or .02% for Run 40 and 26°K or less than 3% for Run 41. Thus we may conclude that the model postulated and the simplifying assumptions made to calculate the substrate temperature are reasonable and well within the uncertainty bounds of the input data (precision of measured source and substrate temperatures, precision of thermodynamic data used etc.)

It would be instructive to compute the error in the deposit temperature for deviations of $\varepsilon_d(T_2)$, $\varepsilon_s(T_2)$ and $\alpha_d(T_2) \times \varepsilon_1(T_1)$ from the values used in the original computation of T_2. This is done in two ways. First, it is assumed that all three parameters $\varepsilon_d(T_2)$, $\varepsilon_s(T_2)$ and $\alpha_d(T_2) \times \varepsilon_1(T_1)$ are off by + 10%, + 20%, - 10% and - 20%. The results are shown in Table V. We note that the largest deviation of the computed T_2 value is only 6%. Secondly, it was assumed that only $\varepsilon_1(T_1)$, the total hemispherical emittance of liquid titanium is off by + 10%, + 20%, - 10%, - 20%. The computed substrate temperature values are only slightly effected.

Calculated Temperature Distribution of Deposit

To compute the temperature distribution from center to edge of the deposit, we need to know the appropriate configuration factors and thickness of the deposit at various points and substitute them into the equation of energy balance. Using the measured thickness of the deposit in Run 40 at various points, the deposit temperature distribution is computed and tabulated in Table VII.

Summary and Conclusions

A model has been proposed for calculating the temperature of the substrate during vacuum deposition. It is based on an energy balance in the substrate-deposit combination. The energy input is from thermal radiation from the evaporation source and from the condensation of metal vapors. The energy loss is by thermal radiation from the substrate and the deposit. Two assumptions were made to simplify the equation of energy balance to permit computation of substrate temperature and comparision with experiments. They were -(1) The "Grey Body" assumption, i.e. spectral emittance is independent of wave-length and -(2) spectral emittance was relatively insensitive to temperature. Computation of substrate temperature agreed very well with the experimentally measured temperature for titanium evaporation. Thus the model and simplifying assumptions appear to be valid.

It is proposed that with this model one can set up evaporation experiments whereby measuring the substrate temperature and other experimental parameters, the total hemispherical emittance of liquid metals can be obtained. Such data is very sparse for liquid metals.

References

1. Bunshah, R. F., and Juntz, R. S., "Electron Beam Distillation Furnace for Reactive Metals: Design Considerations and Operating Experience," Transactions of the Vac. Met. Conf., 1965, American Vacuum Society p. 200.

2. Sparrow, E. M., and Cess, R. D. "Radiation Heat Transfer," Brooks Cole Publishing Company, Belmont, California 1970, p. 117.

3. Edwards, D. W., Denny, V. E., Mills, A. F., "Transfer Process -- An Introduction to Diffusion, Convection and Radiation," Holt, Reinhart and Winston, Inc. - Preliminary Edition, 1970, p. 268.

Appendix 1: Heat transfer due to conduction

We have neglected the mode of energy transfer due to conduction in the equation of energy balance. The following calculation will show that this term is small compared to that due to radiation.

For experiment Run No. 40, we have previously calculated -

$$R_d = 3.76 \times 10^{-2} \times T_2^4 \quad dA_2 \quad \text{ergs} \tag{27}$$

$$R_s = 4.49 \times 10^{-2} \times T_2^4 \quad dA_2 \quad \text{ergs} \tag{28}$$

We consider an area of 5 cm. radius at the center of the deposit and assume that the substrare and deposit radiant at an average temperature of 1/2(895 + 877) = 886°K where 895°K is the center temperature and 877°K is the edge temperature of this 5 cm circular area. Thus, the total energy radiated is

$$R_d + R_s = (8.25 \times 10^{-2}) \times (886)^4 \times \pi \times 25 = 4 \times 10^{12} \text{ ergs} \tag{1'}$$

We define the following terms

E_d = energy transferred by conduction from the center to points 5 cm away in the deposit

E_s = energy transferred by conduction from the center to points 5 cm away in the substrate.

Now,

$$E_d = - K_d \frac{dT}{dr} A_d \quad t \tag{2'}$$

where

K_d = the thermal conductivity of Ti

= 1.72×10^6 ergs/sec cm °K

$\frac{dT}{dr}$ = the temperature gradient from center to points 5 cm away

= $\frac{895-877}{5}$ = 3.6 k°/cm

A_d = the circumferential area of the deposit

= $2\pi \times 5 \times \frac{0.094 + 0.086}{2}$

= 2.82 cm^2

t = duration of the experiment

= 3600 sec.

Substituting all the values into equation (2') we get

$$E_d = - 1.72 \times 10^6 \times 3.6 \times 2.82 \times 3600$$

$$= - 62.9 \times 10^9 \text{ ergs} \qquad (3')$$

Similarly,

$$E_s = - K_s \frac{dT}{dr} A_s \, t \qquad (4')$$

where

K_s = the thermal conductivity

= 2.84×10^6 ergs/sec cm °K

A_s = the circumferential area of stainless steel

= $2\pi \times 5 \times 0.0127$

= 0.4 cm^2

Substituting all values into equation (4'), we get

$$E_s = - 2.44 \times 10^6 \times 3.6 \times 0.4 \times 3600$$

$$= - 11.7 \times 10^9 \text{ ergs} \qquad (5')$$

Thus, the total energy transfer from the center to points 5 cm away due to conduction is $E_d + E_s = -7.46 \times 10^{10}$ ergs.

Since it is less than 2% of the energy due to radiation of the substrate and deposit, we are justified in neglecting it.

TABLE I

Application of Simpson's Rule to Evaluation of $\varepsilon(T_2)$

f	$\frac{hc}{k\lambda T}$	λT	λ at 893°K	$\alpha_d(\lambda)$	Weighting Factor	Product
.1	6.55	2200	2.46	0.31	1	0.31
.3	4.61	3120	3.50	0.26	4	1.04
.5	3.50	4110	4.61	0.23	2	0.46
.7	2.58	5580	6.25	0.20	4	0.80
.9	1.53	9410	10.54	0.18	1	0.15
						+2.76

Hence

$$\varepsilon(T_2) = \int_0^1 \alpha(\lambda)\, df$$

$$= \frac{0.8 \times 2.76}{12}$$

$$= 0.184$$

TABLE II

Experimental Condition for Runs 40 and 41

Run No.	40	41
Melt temperature	2010°C	2010°C
Duration of experiment	60 min.	60 min.
Size of evaporant stock (diameter and height)	3 x 4 in^2	3 x 5 in^2
Collector size	12x12 in^2	12x12 in^2
Collector temperature	620°C	640°C
Distance of collector from source	14.5 in	14.5 in

TABLE III

Thermodynamic and Thermophysical data used in Calculations

Symbol	Measuring	Value	Reference
C_{p_1}	Average heat capacity at constant pressure for Ti vapor between 2283 and 1735°K	5.1×10^6 ergs/gm°K	6
C_{p_2}	Average heat capacity at constant pressure for solid Ti between 1735 and 733°K	6.6×10^6 ergs/gm°K	6
L_s	Latent heat of sublimation of Ti at 1735°K	9.72×10^{10} ergs/gm°K	6
L_t	Latent heat of α-β phase transformation of Ti at 1153°K	8.86×10^8 ergs/gm°K	6
$\varepsilon_s(T_2)$	Total hemispherical emittance of stainless steel at temperature 800-1000°K	0.22	Calculated in this paper
$\varepsilon_d(T_2)$	Total hemispherical emittance of solid Ti at temperature T_2	0.184	Calculated in this paper
$\alpha_d(T_2)$ $\varepsilon_1(T_1)$	Product of total hemispherical absorptance at substrate temperature T_2 and the total hemispherical emittance at source temperature T_1	0.095	Calculated in this paper

TABLE IV

Comparison of Calculated Experimental Values of Substrate Temperature for Titanium Deposition

	Substrate Temperature °K			
	Calculated	Measured	Difference	% Difference
Run 40	895	893	2	0.02
Run 41	887	913	26	2.6

TABLE V

Calculated Substrate Temperature T_2 for Various % Deviations in Values of $\varepsilon_d(T_2)$, $\varepsilon_s(T_2)$, $\alpha_d(T_2)$ X $\varepsilon_1(T_1)$ for Runs 40 and 41 - °K.

	Experimentally Measured	Calculated Values for % Deviations of				
		0%	-10%	-20%	+10%	+20%
Run 40	893	895	915	938	878	865
Run 41	913	887	906	928	871	856

TABLE VI

Calculated Substrate Temperatures T_2 for Various % Deviations in Value of $\varepsilon_1(T_1)$ - the Total Hemispherical Emittance of Liquid Ti source - °K

	Experimentally Measured	Calculated Values for % Deviations of				
		0%	-10%	-20%	+10%	+20%
Run 40	893	895	893	890	898	900
Run 41	913	887	884	882	888	891

TABLE VII

Temperature Distribution of Deposit

Distance away from center	Experimental Value of the thickness	Temperature
0.001 cm	0.094 cm	895°K
5 cm	0.086 cm	877°K
10 cm	0.066 cm	825°K
15 cm	0.043 cm	748°K

SUPPLEMENT-2

Temperature and Thickness Distribution on the Substrate During High Rate Physical Vapor Deposition of Materials

I. INTRODUCTION

High rate physical vapor deposition (HRPVD) is a relatively new technique for synthesis of metals, alloys, ceramics, dispersion strengthened alloys, etc.[1,2,3] Deposition rates of .001 inch (250,000 Å) per minute or greater are obtained. The products which are self-supported structures or thick coatings have practical applications in advanced engineering structures such as honeycomb core material, coatings for jet engine turbine blades, etc. Essentially, the technique consists of two processes; evaporation and condensation . Metals, alloys and ceramics contained in water cooled copper crucibles are evaporated in high vacuum by using high power electron beams. The vapors are collected on heated metallic substrates. The deposition temperature is a very important process parameter. It is desirable to obtain a material of full density and small grain size for high strength and toughness. Bunshah and Juntz[4] have made the following observations. At high deposition temperatures, the material is fully dense but has a large grain size. As deposition temperature decreases the grain size becomes smaller. At very low deposition temperatures, the material is less than full density. Hence it becomes important to deposit at an optimum temperature to obtain fine grain-size fully dense deposits.

In the simple deposition geometry with a flat substrate placed perpendicular to the axis of the vapor source, see Fig. 1, the thickness of the deposit varies from the center to the edges. The thickness gradient and the rate of deposition decrease as the source-substrate distance increases. Therefore, there is an optimum source-substrate distance to obtain the

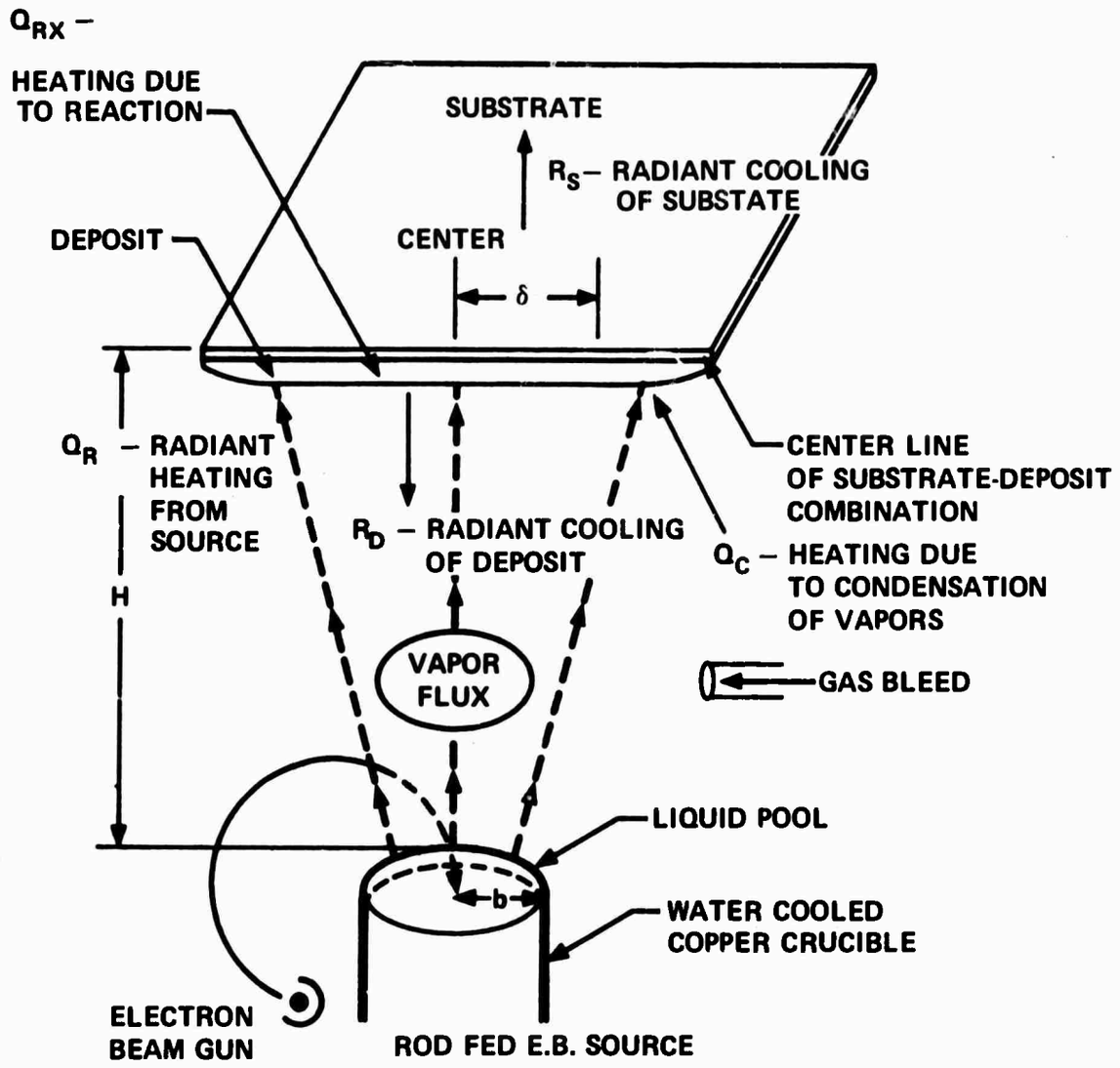

Figure 1. Schematic of High Rate Physical Vapor Process

2.1a

maximum yield of uniform thickness ($\sim$ 5%) deposit consistent with a high deposition rate.

The experimental variables in the high rate physical vapor deposition process are as follows:

1. Nature of the evaporating species (metal, alloy, compound) and the vapor pressure of the component species.
2. Temperature of the source T_1 and the evaporation rate.
3. Thermodynamic properties of condensate (latent heat of condensation, spacific heat, vapor pressure).
4. Heat of reaction in the case of reactive evaporation, e.g. metal vapor plus oxygen reacting to give metal oxide. The reaction may take place on the substrate or in the gas phase.
5. Source diameter.
6. Source to substrate distance, H.
7. Substrate material.
8. Substrate thickness.
9. Size of the substrate.
10. The total hemispherical emittance of the evaporant as a function of evaporation temperature, $\varepsilon_1(T)$.
11. The total hemispherical emittance of the deposit as a function of condensation temperature, $\varepsilon_d(T)$.
12. The total hemispherical emittance of the substrate as a function of condensation temperature, $\varepsilon_s(T)$.
13. The absorptance of the deposit as a function of condensation temperature, $\alpha_d(T)$.
14. The specific heat of the substrate material as a function of temperature.
15. The specific heat of the condensate material as a function of temperature.

II. OBJECTIVE OF THIS INVESTIGATION

With the large number of process variables it is important to be able to focus attention on the range of these variables to be explored experimentally with the objective of obtaining the desired structure in the deposit. To this end, it is the objective of this investigation to illustrate a method for calculating the following:

1. Deposition temperature.
2. Deposition temperature distribution along the substrate.
3. Deposit thickness and its variation along the substrate.

The deposition of yttrium and yttria (Y_2O_3) by evaporation from a liquid yttrium source will be used to illustrate the method. Y_2O_3 is formed by reactive evaporation of Y vapors in the gas phase or on the substrate with O_2 introduced into the gas phase. The results of the calculations will yield the specific range of variables to be explored experimentally.

Radiation from the source, energy liberated by the condensation of metal vapors and the heat of reaction for reactive evaporation are the sources heating the substrate. Their relative importance for various experimental conditions will be evaluated.

III. CALCULATIONS

Calculations will be made for the following range of experimental variables.

1. Temperature of the liquid Y source 2,200, 2,300, 2,400°K (M.P. of Yttrium is 1768°K).
2. Source diameter - 1.0 and 1.5 inches.
3. Source to substrate distance - 10, 15, 25, 50 cm.
4. Substrate materials - copper, stainless steel.

5. Substrate thickness - 0.001, 0.005, 0.01, 0.05 inch.

6. Substrate size (diameter) - 8, 16, 24 cm.

A. Vapor Pressure and Evaporation Rate

Vapor pressure data are given in the following form

$$\text{Log}_{10} P = A\, T^{-1} + B \log_{10} T + CT + DT^2 + E$$

where

P = vapor pressure of the metal, torr

T = temperature of the metal, °K

A,B,C,D, and E = constants, characteristic of the metal

Evaporation Rate

The evaporation rate of a metal is governed by Langmuir equation

$$G = K\, P\, (M/T)^{1/2}$$

where

G = weight evaporated, g/cm^2-sec.

P = vapor pressure, torr.

T = temperature of the metal, °K.

M = molecular weight of the gas phase

K = constant = 0.05833

The vapor pressure and evaporation rate of yttrium at various temperatures are calculated and tabulated in Appendix-1. Evaporation rate of yttrium with temperature is plotted in Fig. 2.

B. Temperature and Temperature Distribution of the Substrate

The experimental set-up for high rate plysical vapor deposition processes (HRPVD) is shown in Figure 1. The metal is contained in a water-cooled copper crucible heated by an electron beam source. The metal vapors are condensed on a metallic substrate located above the source.

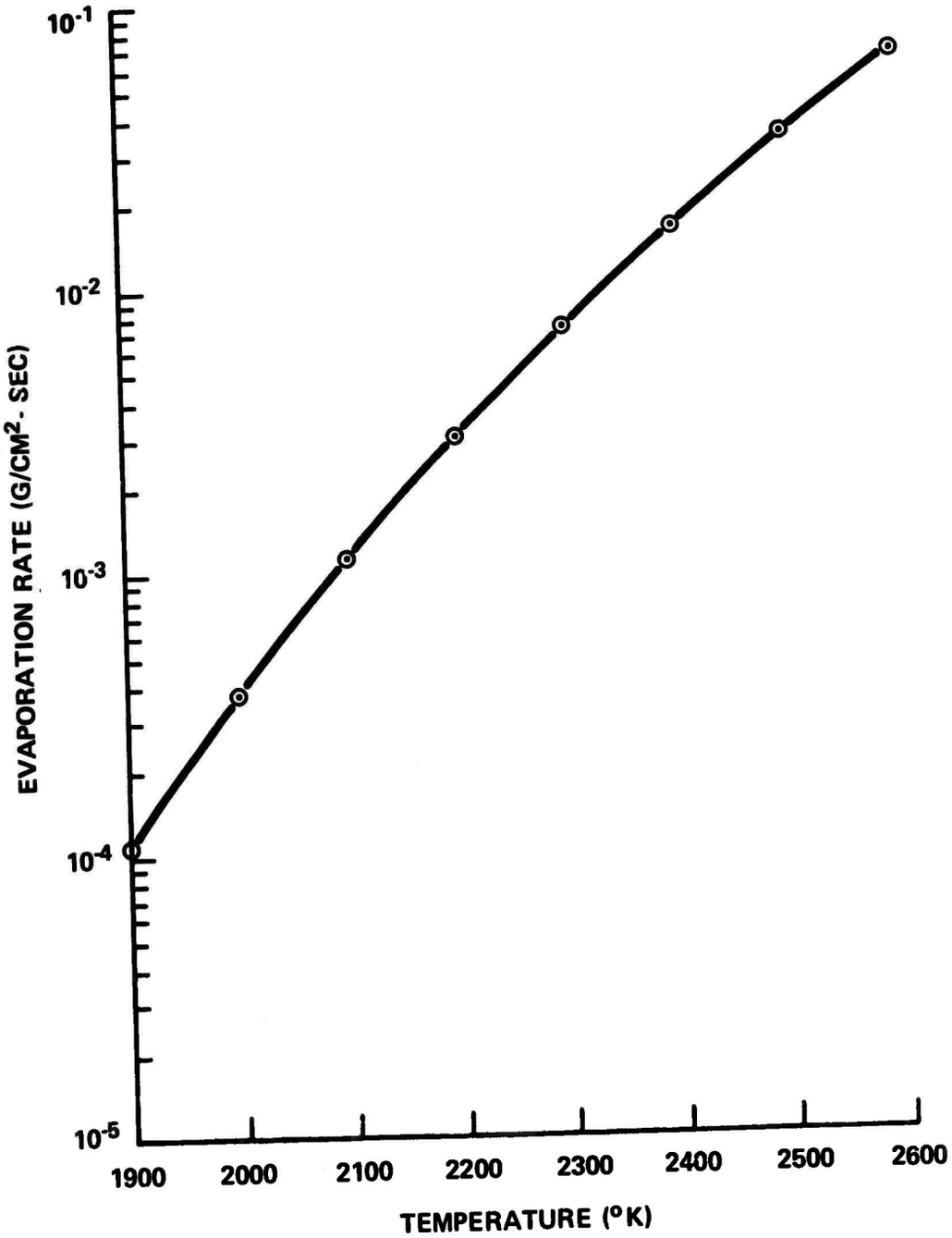

Figure 2a. Evaporation Rate of Yttrium vs Temperature

The model for calculation of the substrate temperature is based on the energy balance between the energy input and output of the substrate.

The energy input to the substrate consists of three terms:

Q_R - the radiant energy from the source at temperature T_1

Q_C - energy supplied by the condensation of metal vapors

Q_{Rx} - the heat of reaction for reactive evaporation i.e., if a reaction occurs between the condensing vapors and a gas phase on the substrate or between two metal vapors condensing on the substrate. For simple condensation of metal or alloy vapors this term is zero.

The energy output from the substrate consists of the following terms:

R_d - energy radiated from the deposit at temperature T_2 of the substrate

R_s - energy radiated from the back side of the substrate at temperature T_2 i.e., the side away from the source

H_s - energy necessary to heat the substrate from the initial temperature T_3 to the final temperature T_4 in any interval of time

H_d - energy necessary in the n^{th} interval to heat material deposited in the (n-1) intervals.

We can now write the equation of energy balance as:

$$Q_R + Q_C + Q_{Rx} = R_d + R_s + H_s + H_d \qquad (1)$$

Initially during the process, the energy input will exceed the heat output and the temperature of the substrate-deposit combination will rise; thus causing an increased energy loss from the substrate. The starting temperature of the substrate is assumed to be 300°K. Next, time is divided into intervals of 10 seconds and using equation 1 above, the temperature rise in the substrate-deposit combination is computed for each interval. The final temperature of each interval is taken as the starting temperature of the following one. Since the energy input to the substrate deposit combination is constant and the output is proportional to T_2^4 (T_2 being the substrate temperature), a steady state will be reached. Under steady

state conditions, H_s and H_d in equation 1 are zero and the equation of energy balance becomes

$$Q_R + Q_c + Q_{Rx} = R_d + R_s \qquad (2)$$

The validity of this model has been confirmed by Chow and Bunshah[5] by comparing the computed and measured substrate temperatures for titanium evaporation. In further calculations, the following assumptions were made:

1. The surface of the evaporating source is flat and at a uniform temperature.
2. Heat loss by conduction on the substrate is negligible, as shown by Chow and Bunshah.[5]
3. The surface of the deposit behaves like a gray body and hence spectral absorptance is equal to the spectral emittance. This assumption is often used in radiant heat transfer calculations[6]. Its validity has been tested by Chow and Bunshah[5] for the deposition of titanium.
4. The substrate has black body surroundings at a constant temperature of 300°K.
5. The deposit has theoretical density.

Let us now examine in detail each of the terms in Equation (1).

Q_R - Energy gain due to radiation from the source.

Heat absorbed by an infinitesimal area dA_2 on the substrate due to radiation from the source of area A_1 and using the reciprocity relationship shown later in eq. 9, we get:

$$Q_R = \sigma \, dA_2 \; \varepsilon_1(T) \; \alpha_d(T) \; F_{dA_2-A_1} \; T_1^4 \qquad (3)$$

where

σ = Stefan-Boltzmann Constant, cal/°K^4-sec.-cm.^{2}

$\varepsilon_1(T)$ = Total hemispherical emittance of the source

$\varepsilon_d(T)$ = Total hemispherical emittance of the deposit

$\alpha_d(T)$ = Total hemispherical absorptance of the condensate

T_1 = Temperature of the source, °K.

$F_{dA_2-A_1}$ = Configuration factor for radiation going from area dA_2 to area A_1.

It is assumed that the absorbtance of the deposit has to be taken as that of the substrate until 50 atomic or molecular layers are deposited. The times to achieve this condition for the experimental conditions under investigation have been calculated and given in Appendix-2. The times are too small compared to the duration of the experiments and hence are neglected.

Q_c-Energy gain due to condensation of vapors

Energy given to an infinitesimal area dA_2 on the substrate due to condensation of vapors is:

Q_c = number of moles condensing x heat of condensation per mole.

The number of moles condensing per second

$$= \frac{G}{M} \; dA_2 \; F_{dA_2-A_1}$$

where M = molecular weight

G = evaporation rate, $g/cm^2 sec$

Heat of condensation per mole

= $(H_{T_1} - H_{298})_{vapor}$ + heat of sublimation at 298°K

- heat required to heat Y from 298°K to the substrate temperature T_2

where

$(H_{T_1} - H_{298})_{vapor}$ = enthalphy change in vapor from T_1 to 298°K.

Let

F = $(H_{T_1} - H_{298})_{vapor}$ + heat of sublimation at 298°K.

The values of F are computed as a function of source temperature and given in Appendix 3.

Heat required to heat one mole of yttrium from 298°K to the substrate temperature T_2

= molar specific heat x $(T_2 - 298)$

$$= (5.59 + 1.9 \times 10^{-3} \times T_2 + \frac{0.29 \times 10^5}{T_2^2})(T_2 - 298)$$

$$= 5.0238 \times T_2 + 1.9 \times 10^{-3} \times T_2^2 + \frac{0.29 \times 10^5}{T_2} - \frac{86.42 \times 10^5}{T_2^2} - 1665.82$$

$$\therefore Q_c = \frac{G\, dA_2 F_{dA_2 - A_1}}{M} \{F - 5.0238 \times T_2 - 1.9 \times 10^{-3} \times T_2^2 - \frac{0.29 \times 10^5}{T_2} + \frac{86.42 \times 10^5}{T_2^2} + 1665.82\} \text{cal/sec.} \quad (4)$$

$\underline{Q_{Rx}}$ - Heat gain due to Reaction

The model assumed for the deposition of yttria is that yttrium vapors condense on the substrate and then react with gaseous oxygen to form solid yttria:

$$Y_{vapor} \longrightarrow Y_{solid}$$

$$2Y_{(solid)} + \frac{3}{2}\, O_{2(gas)} \longrightarrow Y_2O_{3(solid)}$$

Since, heat of reaction is a thermodynamic state property, even if metal vapors react with oxygen gas in the vapor phase to form oxide and then condense to solid yttria, the heat of reaction will be the same.

Heat given to an infinitesimal area dA_2 on the substrate due to the formation of yttria:

Q_{Rx} = number of moles of yttria formed x heat generated per mole.

The number of moles of yttria being formed per second

$$= \frac{G\, dA_2\, F_{dA_2 - A_1}}{2M}$$

Heat generated per mole is equal to

$$\Delta H_{298°K} + \int_{298}^{T_2} \Delta Cp\, dT$$

where

ΔH_{298} = Enthalpy of reaction at 298°K, cal/mole.

$$\Delta C_p = C_{p_{Y_2O_3}} - 2\,C_{p_{y(s)}} - \frac{3}{2}\,C_{p_{O_2\,(g)}}$$

$$= 7.68 - 4.1 \times 10^{-3} \times T_1 - \frac{4.76 \times 10^5}{T_1^2}$$

$$\int_{298}^{T_2} \Delta C_p = 7.68 \times T_2 - 2.05 \times 10^{-3} \times T_2^2 + \frac{4.76 \times 10^5}{T_2} - 3706.60$$

$$\therefore Q_{Rx} = \frac{G\,dA_2\,F_{dA_2-A_1}}{2M} \left\{ 459,106.60 - 7.68 \times T_2 + 2.05 \times 10^{-3} \times T_2^2 - \frac{4.76 \times 10^5}{T_2} \right\} \text{ cal/sec.} \quad (5)$$

R_s - Heat Loss Due to Radiation from Substrate

The heat loss due to radiation from the substrate to the surroundings, from an area dA_2,

$$R_s = \sigma\,\varepsilon_s(T)\,(T_2^4 - 300^4)\,dA_2 \text{ cal/sec.} \quad (6a)$$

where

$\varepsilon_s(T)$ = total hemispherical emittance of the substrate

R_d - Heat Loss due to Radiation from the Deposit

The heat loss due to radiation from the deposit to the surroundings, from an infinitesimal area dA_2,

$$R_d = \sigma\varepsilon_d(T)\,(T_2^4 - 300^4)\,dA_2 \text{ cal/sec.} \quad (6b)$$

H_s - Heat required to heat the substrate from the starting temperature (T_3) of an interval to the final substrate temperature (T_4) of the interval.

The heat required to heat an element of substrate of area dA_2 from the starting temperature of the interval (T_3) to the final temperature of the interval (T_4),

H_s = mass x specific heat x (T_4-T_3)

= thickness x density x dA_2 x specific heat x (T_4-T_3) (7)

H_d - Heat required in the n^{th} interval to heat the condensate deposited in the prior (n-1) intervals from the starting (T_3) to the final (T_4) temperature of the interval

For the deposition of yttrium,

H_d = number of moles of Y deposited in (n-1) intervals in an area dA_2 x molar specific heat of Y x (T_4-T_3)

$$= \frac{G}{M}\, dA_2\, F_{dA_2-A_1}\, (n-1) \quad [5.59 \times T_4 + 1.9 \times 10^{-3} \times T_4^{\,2} + \frac{0.29 \times 10^5}{T_4} - 5.59 \times T_3 - 1.9 \times 10^{-3} \times T_3 \times T_4 - \frac{0.29 \times 10^5 \times T_3}{T_4^{\,2}}] \qquad (8a)$$

For the deposition of yttria,

H_d = number of moles of yttria deposited in (n-1) intervals in an area dA_2 x molar specific heat of yttria x $(T_4 - T_3)$

$$= \frac{G}{2M}\, dA_2\, F_{dA_2-A_1}\, (n-1)\, [29.60 \times T_4 + 1.20 \times 10^{-3} \times T_4^{\,2} - \frac{4.78 \times 10}{T_4} - 29.60 \times T_3 - 1.20 \times 10^{-3} \times T_3 \times T_4 + \frac{4.78 \times 10^5 \times T_3}{T_4^{\,2}}] \qquad (8b)$$

Computation of the Substrate Temperature T_2

Substituting the above equations 3,4,5,6,7,8 representing the various terms into the equation of energy balance (eq. 1), it assumes the form:

$$T_2^{\,4} + A_5 \times T_2^{\,2} - \frac{A_6}{T_2^{\,2}} + A_7 \times T_2 + \frac{A_9}{T_2} - A_{10} = 0$$

where, A_5, A_6, A_7, A_9 and A_{10} are material constants.

An equation of this form is solved for T_2 by Newton-Ralphson method[10] which is as follows:

$$f = T_2^{\,4} + A_5 \times T_2^{\,2} - \frac{A_6}{T_2^{\,2}} + A_7 \times T_2 + \frac{A_9}{T_2} - A_{10}$$

$$f' = 4 \times T_2^{\,3} + 2 \times A_5 \times T_2 + \frac{2 \times A_6}{T_2^{\,3}} + A_7 - \frac{A_9}{T_2^{\,2}}$$

Initially, T_2 is given an arbitrary value, say T_2'. Then a new value of T_2 is found, e.g., T_2 new = $T_2' - (f/f')$. This new value is substituted in place of T_2' and another new value is found. This process is repeated until T_2 new - T_2' is within the limits of accuracy desired (1.0% is sufficiently accurate for our calculations).

A computer program has been developed to compute the temperature on the substrate at various points, as a function of experimental variables. The temperature variation is plotted in figures 3 & 4 and tabulated in tables I and II.

The data used in these calculations is given in Table XIII along with the symbols and sources of data. Since no values were available for the total hemispherical emittance of Y, the spectral value at $\lambda = 0.65\mu$ is used instead. Similarly for the total hemispherical absorbtance of Y_2O_3, the spectral value at $\lambda = 0.65\mu$ for oxidized yttrium is used. Changes in the computed substrate temperature T_2 for deviations from the assumed values of emittance and absorbtance are calculated and discussed below.

C. Thickness Distribution on the Substrate

The mass of yttrium reaching an infinitesimal area dA_2 on the substrate, from the source is equal to;

$$G\, A_1\, dF_{A_1-dA_2}$$

where

A_1 = surface area of the source, cm^2

Using the reciprocity relation of configuration factors,

$$G\, A_1\, dF_{A_1-dA_2} = G\, dA_2\, F_{dA_2-A_1} \qquad (9)$$

where $dF_{A_1-dA_2}$ = configuration factor to dA_2 from the source of surface area A_1.

$$F_{dA_2-A_1} = \frac{1}{2}\left(1 - \frac{Z - 2Y^2x^2}{\sqrt{Z^2 - 4\,Y^2x^2}}\right)$$

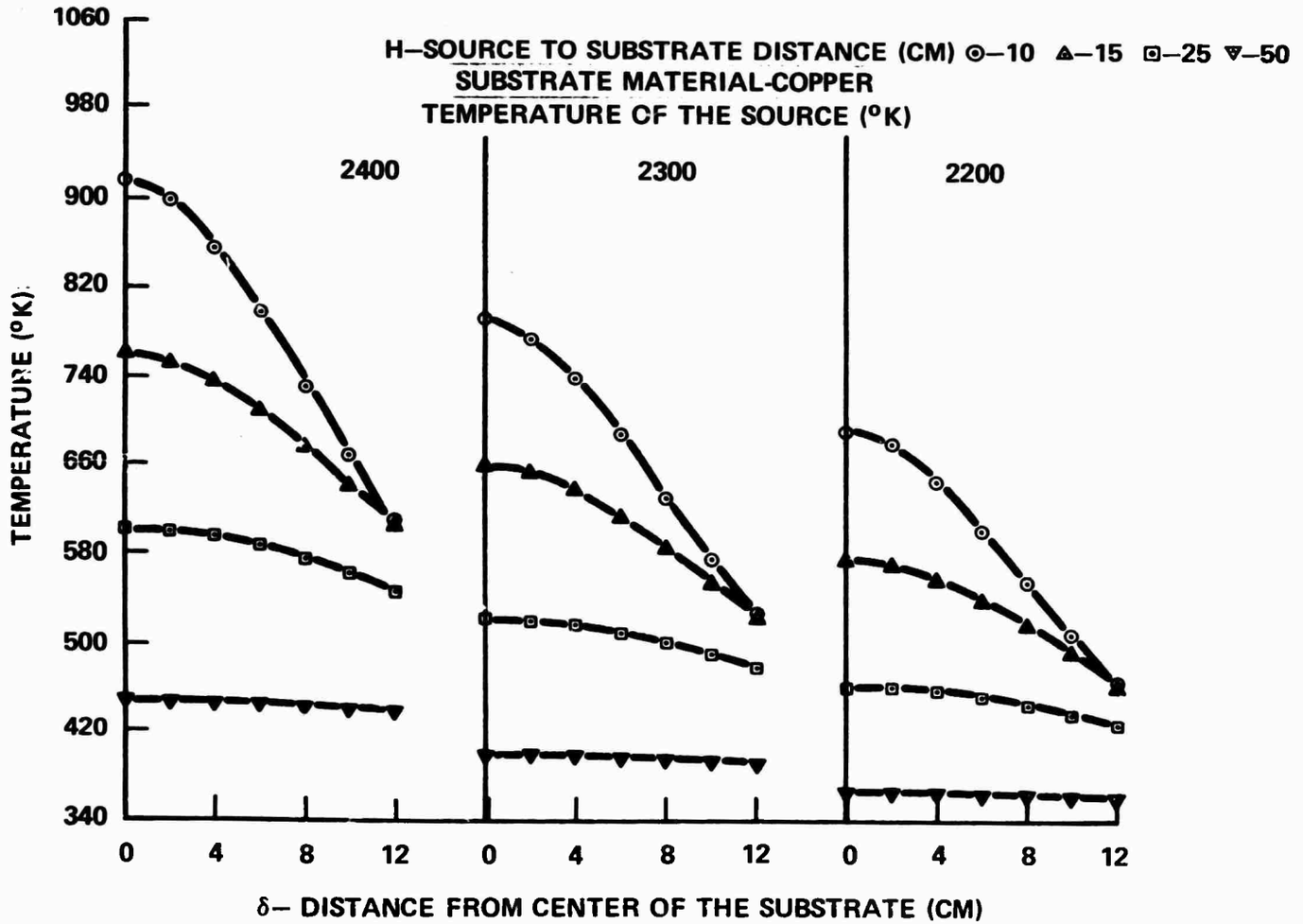

Figure 3. Temperature Variation for the Deposition of Yttrium

2.11a

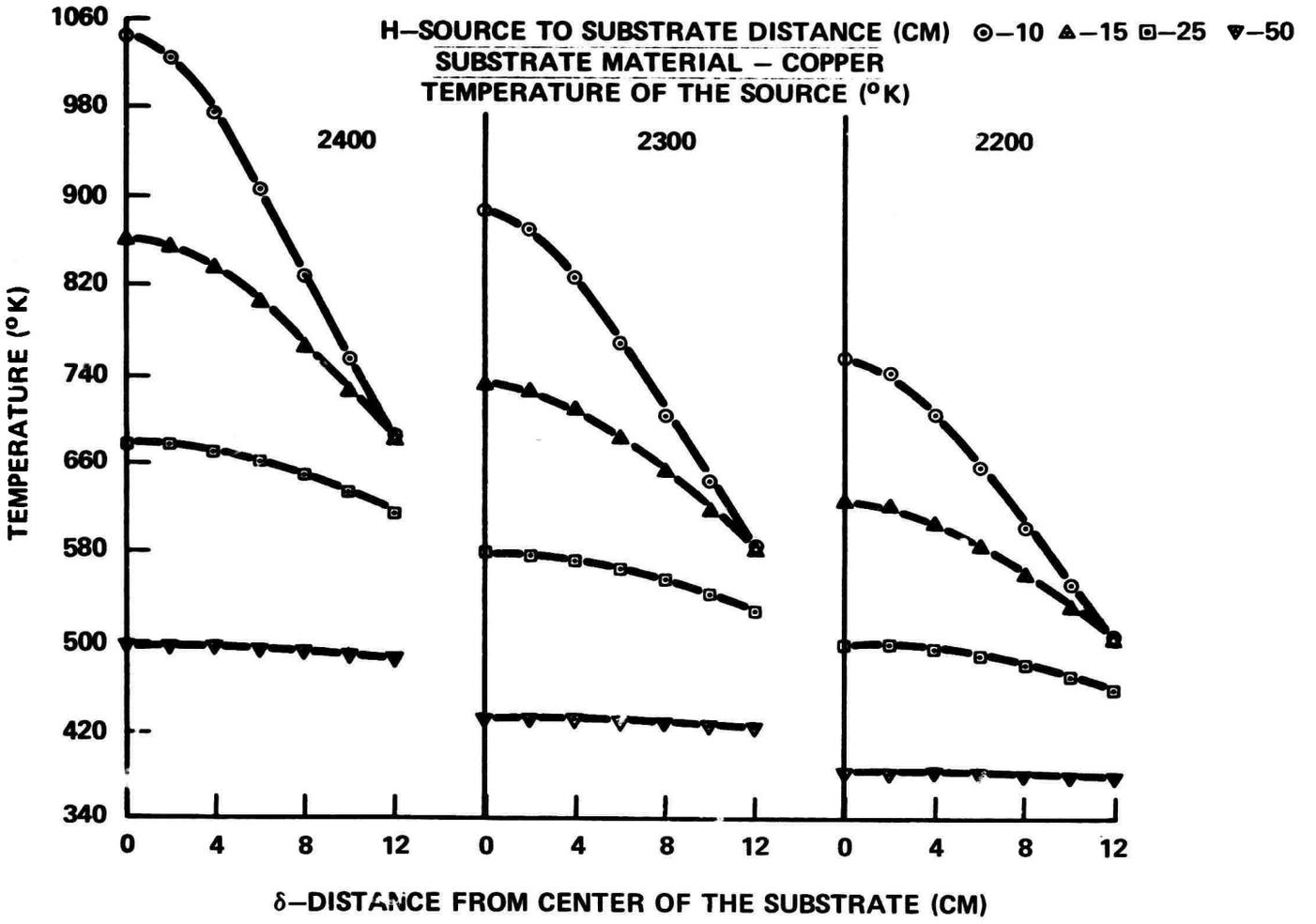

Figure 4. Temperature Variation for the Deposition of Yttria

where $Z = 1 + (1+Y^2)\ x^2$

$Y = b/H$

$x = H/\delta$

and δ, b, and H are shown in figure 1.

The thickness at any point on the substrate is calculated by using the mass balance equation

$$G\ dA_2\ F_{dA_2-A_1} = \tau\ dA_2\ \rho$$

where τ = thickness of the condensate at any point, cm

ρ = density of the deposit, g/cm^3

$$\therefore \tau = \frac{G\ F_{dA_2-A_1}}{\rho}\ cm. \qquad (10)$$

The calculated thickness values are shown in figure 5 and Table III.

IV. DISCUSSION OF RESULTS

The results of the computations will be discussed under four principal headings:

A. Effect of Experimental Variables on Temperature and Thickness Distribution on the Substrate.

B. Time to Reach Steady State Temperature as a Function of Substrate Thickness.

C. Errors in Substrate Temperature Calculations due to Deviations in the Assumed Emittance Values for Source and/or Substrate Materials and of the Surroundings.

D. Relative Contribution of Various Energy Sources in Heating the Substrate.

The discussion is as follows:

A. Effect of Experimental Variables on the Temperature and Thickness Distribution on the Substrate.

1. Source Temperature - Referring to tables I, II, & III as the temperature of the source increases, the evaporation and the deposition rates of the metal increase. Thus, the deposition rate at 2300°K is 2.5 times and that at 2400°K is 5.5 times the deposition rate at 2200°K. The temperature on the substrate increases with increasing source temperature. The

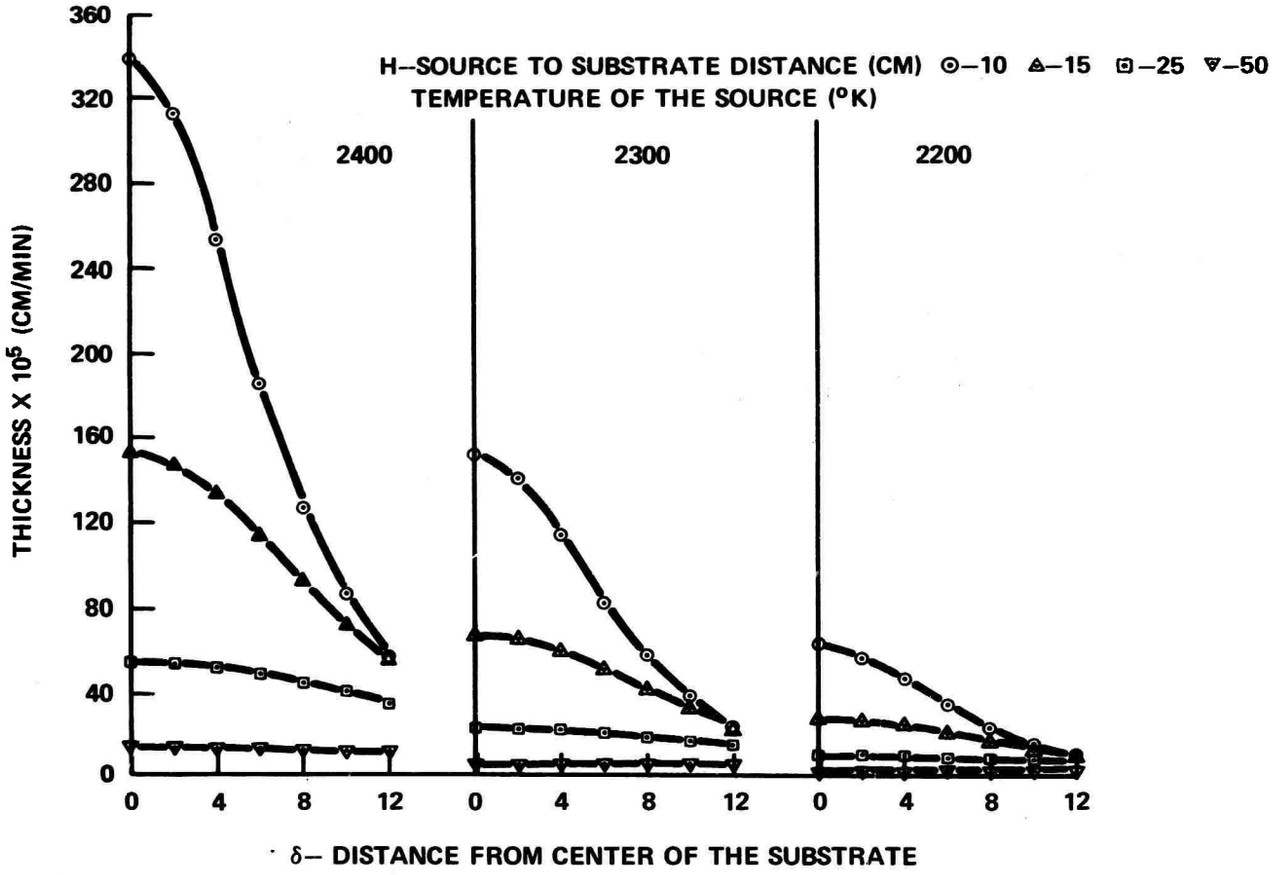

Figure 5. Thickness Variation for the Deposition of Yttrium

2.12-4

corresponding temperatures for the deposition of yttria are higher than those for the deposition of yttrium. The percent thickness and temperature variation from the center to the edges of the deposit is independent of the source temperature. The percent temperature variation is only about 1% higher for the deposition of yttria, than for yttrium.

2. Source to substrate distance - As the distance between the source and the substrate is increased, the deposition rate and the temperature at each point of the substrate decrease considerably. But, the percent thickness and temperature variation also decreases. In other words, as the source-substrate distance is increased, the deposit becomes more and more uniform in temperature and thickness and hence in structure and mechanical properties. The temperature variation along the deposit for both yttria and yttrium is about same, as seen in tables I, II, & III. The corresponding substrate temperatures for yttria are higher than those for yttrium.

3. Diameter of source - The thickness and temperature at each point on the deposit increase with increasing diameter of the source. Thus, from table III, the deposition rate with 1.5" source is twice that with a 1.0" diameter source. But the percent thickness and temperature variation on the substrate is independent of the source diameter.

4. Substrate size - As the diameter of the substrate increases, the thickness and temperature difference between the center and the edges increase. Thus, the thickness variations from the center to the edge are 25, 60, and 80% for 8, 16, and 24 cm. diameter substrates respectively, for a source to substrate distance, H, of 10 cm. Of course, this variation becomes less with increasing H. Similarly, as can be seen from tables I & II the percent temperature difference between the center and the edges increases with the substrate size for the deposition of both yttrium and yttria.

5. Substrate material - The temperature at each point with a copper substrate is higher than that with stainless steel substrate. This is due to the lower emittance of copper as compared to stainless steel. The percent temperature difference for the two substrate materials increases with increasing substrate temperature and varies from 4 to 10%, for the deposition of yttrium. It would be higher for yttria deposition because of higher substrate temperatures. The results are given in Table IV.

B. Time to Reach Steady State Temperature as a Function of Substrate Thickness

The time to reach steady state temperature increases markedly with increasing substrate thickness, as can be seen in tables V & VI. The time decreases considerably with increasing source temperature, but increases with increases H. The corresponding times for yttria are much smaller than for yttrium, especially at greater substrate thicknesses.

C. Errors in Substrate Temperature Calculations due to Deviations in the Assumed Emittance Values of the Source and/or Substrate Materials

1. Deviations of source and deposit emittances taken together -

Temperature distribution for the deposition of yttrium and yttria are calculated for various emittance values of the condensate and the evaporant and are tabulated in tables VII & VIII. As the deviation in emittances increases the errors in calculated temperatures increase at source temperature 2200°K for the deposition of yttrium. But for a source temperature of 2400°K, and hence a much larger evaporation and deposition rates, there is negligible error, less than 1%, even for the largest possible error in emittances considered. For the deposition of yttria, the errors are in a much closer range of 2 to 5%.

2. Deviations of substrate emittance values only - Temperatures on the substrate are calculated for buffed stainless steel substrate and rolled stainless steel substrate and are tabulated in table IX. The rolled substrate

has 1.5 to 2 times higher emittance than buffed substrate and hence gives rise to 5 to 8% lower temperatures than the latter. The temperature of the source and the distance between the source and the substrate do not seem to influence the difference considerably.

3. Deviations in Emittance of the Surroundings of the Substrate

Emittance values of the surroundings are varied from 0 to 1 and the substrate temperatures calculated are given in table X. It is observed that when the substrate temperature is greater than 450°K, the errors in temperatures due to errors in the emittance of the surroundings are very small. As the temperatures of the substrate increase, the errors become less. Around 500°K, the error is only 2% even when the emittance of the surroundings varies from 0 to 1. At 600°K, it is 1% and at 700°K, it is < 1%.

D. Relative Contributions of Various Energy Sources in Heating of the Substrate

The various energy sources contributing to the heating of the substrate are the radiant energy from the source, the energy due to condensation of the vapors, and that due to the heat of reaction (applies to yttria only). Their relative contributions are calculated for various experimental conditions for the deposition of yttrium and yttria and are given in tables XI and XII. They are a function of the material being deposited and the temperature of evaporation. For the deposition of yttrium, radiation from the source contributes twice that for condensation at 2100°K; contributions are almost equal at 2200°K. At 2300°K, the contribution of condensation is twice that due to radiation and at 2400°K, the former contributes about 3.5 times the latter. Thus, we see that there is a reversal of relative contributions above a source temperature of 2200°K. The relative contribution is insensitive to the distance between the source and the substrate.

For the deposition of yttria, at 2000°K, radiation contributes 10 times that due to condensation and 5 times that due to reaction. As the temperature of the source increases, the relative contributions vary. Thus, at 2200°K, radiation contributes two times the condensation and same as that due to reaction. Relative contributions of radiation and condensation are equal and reaction contributes two times either one at 2300°K. Finally, at 2400°K, condensation contributes two times and the reaction contributes four times that due to radiation.

V. SUMMARY AND CONCLUSIONS

Temperature and thickness variation on the substrate for the deposition of yttrium and yttria are computed for various experimental conditions. Temperature of the source, diameter of the source, source to substrate distance, material of the substrate and the thickness of the substrate are the important variables in these experiments.

There are three sources of heat input to the substrate, viz. radiation from the source, condensation and reaction. The relative contribution of these sources is calculated for various experimental conditions. Probable errors in temperatures of the substrate due to deviations in the assumed emittance values of the substrate material, condensate and the source are estimated.

One of the stated objectives at the start of this paper was to use the computations to focus on the range of variables to be explored experimentally. Let us now set some criteria for the production of a desirable deposit at high deposition rates, .0001-.001" per minute. Such a deposit should be of full density and have a reasonably uniform microstructure (i.e. variation in deposition temperature up to 5%) and thickness uniformity ($\leq$ 5% from center to edge).

From the calculations and discussion above, one would focus on the following range of variables to be explored experimentally.

1. Temperature of the source - 2300 to 2600°K
2. Source to substrate distance - 25 to 35 cm.
3. Diameter of source - 1.0" to 1.5".
4. Substrate material - buffed stainless steel and copper.
5. Substrate thickness - .001 to .005".
6. Substrate size (diameter) - 8 to 20 cm.

These criteria represent compromises between the possible extremes. For example, one can get great thickness uniformity by making the source-to-substrate large but at the expense of deposition rate and substrate temperatures which may be too low to produce a fully dense structure. Furthermore, the data shows that errors in substrate temperature estimates are only slightly influenced by variations in source or substrate material emittances by operating at high source temperatures, which also gives high deposition rates. The computations also illustrate what substrate temperatures and thickness distributions to expect in case certain experimental parameters are fixed or beyond one's control. In such cases, one might resort to other methods to enhance substrate temperature and thickness uniformity[7], e.g. preheating of the substrate, beam-sweep on a variable residence time/intensity pattern in a rectangular electron beam source etc.

REFERENCES

1. Bunshah, R. F., and Juntz, R. S., Trans. Vac. Met. Conf., 1965, American Vacuum Society, p. 200.

2. Bunshah, R. F., and Juntz, R. S., Trans. Vac. Met. Conf., 1966, AVS, p. 209.

3. Smith, H. R., et al., Journal of Vac. Sci. & Tech., 7, S48, 1970.

4. Bunshah, R. F., and Juntz, R. S., to be published.

5. Chow, R., and Bunshah, R. F., Supplement I, this report.

6. Sparrow, E. M., and Cess, R. D., "Radiation Heat Transfer," 1970, p. 117.

7. Bunshah, R. F., and Juntz, R. S., Trans. Vac. Met. Conf., 1967, AVS, p. 799.

8. Honig, R. E., and Kramer, D. A., "Vapor Pressure Data for the Solid and Liquid Elements," Techniques of Metals Research, Ed. R. F. Bunshah, Vol. IV, pt. 1, 1970, p. 505.

9. Cullity, B. D., "Elements of X-Ray Diffraction," Addison-Wesley Pub. Co., Inc. 1967, p482.

10. Ralston, Anthony, "A First Course in Numerical Analysis," McGraw-Hill Book Company, 1965, p. 329.

11. Kubaschewski, O., et al., "Metallurgical Thermochemistry," Pergamon Press, Oxford, 4th Ed., 1967, p. 388.

12. Hultgren, R., et al., "Selected Thermodynamic Properties of Metals and Alloys," J. Wiley & Sons, N.Y., 1963, p. 312.

13. Handbook of Chemistry and Physics, CRC, 50th Ed., 1969-70.

14. McElroy, D. L., and Fulkerson, W., "Temperature Measurement and Control," Techniques of Metals Research, Ed., R.F. Bunshah, vol. 1, pt. 1., 1968, p.209.

15. Smithels, C. J., "Metals Reference Book," 4th ed., New York, Plenum Press, 1967, vol. 3, p. 727.

16. Goldsmith, et al., "Handbook of Thermophysical Properties of Solid Materials," 1961, II-D-2.

17. Kubaschewski, O., et al., "Metallurgical Thermochemistry," Pergamon Press, Oxford, 4th ed., p. 396.

18. ibid., p. 360.

19. Metals Hand-Book, ASM, 8th Ed., Vol. 1, 1969, p. 425.

Appendix - 1

Vapor Pressure and Evaporation Rate of Yttrium

Vapor Pressure Constants[β]:

$$\log_{10} P = AT^{-1} + B \log_{10} T + CT + DT^2 + E$$

$A = -25.2380 \times 10^{3}$

$B = -3.22193$

$C = -1.18490 \times 10^{-3}$

$D = 1.64376 \times 10^{-7}$

$E = 23.4525$

Temperature °K	Vapor Pressure (mm)	Evaporation Rate g/cm^2-sec.
2,000	0.305687×10^{-1}	0.375939×10^{-3}
2,100	0.926585×10^{-1}	0.111207×10^{-2}
2,200	0.251396×10^{0}	0.294783×10^{-2}
2,300	0.620095×10^{0}	0.711130×10^{-2}
2,400	0.140913×10^{1}	0.158198×10^{-1}

Appendix - 2

Time to deposit 50 atomic or molecular layers on the substrate

Atom Size[9] of Yttrium = 3.60 A°

Equivalent thickness of 50 atoms = 1.8×10^{-6} cm.

Time to achieve 50 atomic layers

$$= \frac{1.8 \times 10^{-6}}{\text{condensation rate}} \text{ sec.}$$

For example

At source temperature of 2200°K,

H = 10 cm, Delta = 0

$$\text{Time} = \frac{1.8 \times 10^{-6}}{1.07 \times 10^{-5}}$$

$$= \underline{0.168 \text{ sec}}.$$

		Temperature of the Source °K			
		2200		2300	
H(cm)	Delta (cm)	Thickness rate cm/sec.	Time (sec)	Thickness rate cm/sec.	Time (sec)
10	0	1.07×10^{-5}	0.17	2.58×10^{-5}	0.07
15	0			1.15×10^{-5}	0.16
25	0	0.171×10^{-5}	1.05	0.413×10^{-5}	0.44
	6	0.153×10^{-5}	1.18	0.369×10^{-5}	0.49
50	0	0.427×10^{-6}	4.2	0.103×10^{-5}	1.75

Appendix - 3

Heat of Condensation at 298°K for Yttrium

Heat of Sublimation[11] at 298°K = 101.5 $\pm$ 2.0 K cal/mole.

$F = (H_T - H_{298})_{vapor} +$ heat of sublimation at 298°K.

Temperature °K	$(H_T - H_{298})^{12}_{vapor}$ cal/mole	F cal/mole
1700	7559	109059
1900	8590	110090
2000	9111	110611
2100	9641*	111141
2200	10172	111672
2300	10720*	112220
2400	11267	112767
2600	12410	113910

*Interpolated

LIST OF TABLES

TABLE I

Effect of Change of Source Diameter and Temperature on Substrate Temperature Distribution for the Deposition of Yttrium

Source to Substrate Distance (cm)	Delta (cm)	Temperature of the Source (°K) 2200 Diameter of the Source 1.0" Temp.°K	%Temp. Variation	1.5" Temp.°K	%Temp. Variation	2300 Diameter of the Source 1.0" Temp.°K	% Temp. Variation	1.5" Temp.°K	%Temp. Variation	2400 Diameter of the Source 1.0" Temp.°K	%Temp. Variation	1.5" Temp.°K	%Temp. Variation
10	0	631.1		753.0		718.2		857.5		826.2		986.1	
	4	592.3	6.2	707.3	6.1	673.3	6.25	805.4	6.1	774.4	6.25	926.4	6.05
	8	511.8	18.9	609.4	19.1	579.4	19.4	693.1	19.2	665.0	19.5	797.3	19.1
	12	437.4	30.6	514.5	31.8	490.2	31.8	582.7	32.1	559.3	32.3	668.3	32.1
15	0	530.3		631.1		601.2		718.2		690.6		826.2	
	4	515.4	2.81	612.8	2.9	583.7	2.92	697.1	2.94	670.1	2.97	801.9	2.94
	8	478.7	9.73	567.1	10.1	540.2	10.15	644.1	10.3	618.9	10.4	740.6	10.35
	12	435.7	17.8	511.8	18.9	488.2	17.9	579.4	19.3	556.8	19.3	665.9	19.5
25	0	432.9		507.6		484.7		574.4		552.6		659.2	
	4	428.9	0.93	502.3	1.03	479.8	1.01	568.2	1.08	546.7	1.07	651.9	1.1
	8	418.0	3.45	487.8	3.9	466.2	3.82	551.0	4.08	530.2	4.05	631.7	4.18
	12	402.6	7.0	467.0	8.0	446.9	7.8	526.1	8.43	506.5	8.35	602.2	8.65
50	0	350.9		392.2		378.8		433.6		419.6		490.0	
	4	350.4	0.14	391.4	0.20	378.1	0.18	432.6	0.23	418.7	0.22	488.7	0.27
	8	349.0	.54	389.0	0.82	376.0	0.74	429.6	0.92	415.9	0.89	485.0	1.02
	12	346.6	1.23	385.4	1.73	372.7	1.61	424.9	2.0	411.5	1.93	479.1	2.22

TABLE II

Temperature Distribution on the Substrate for the Deposition of Yttria

Source to Substrate Distance (cm)	Delta (cm)	Temperature of the Source °K: 2200 Temp. °K	2200 Difference	2200 % Difference	2300 Temp. °K	2300 Difference	2300 % Difference	2400 Temp. °K	2400 Difference	2400 % Difference
10	0	708.4			826.8			968.8		
	4	663.2	45.2	6.4	773.5	53.3	6.45	906.4	62.4	6.45
	8	568.9	139.5	19.7	661.6	165.2	20.0	774.5	194.3	20.1
	12	480.5	227.9	32.1	554.3	272.5	33.0	646.3	322.5	33.4
15	0	590.8			687.7			805.3		
	4	573.2	17.6	2.98	666.8	20.9	3.04	780.6	24.7	3.06
	8	529.9	60.9	10.3	614.7	73.0	10.6	718.7	86.6	10.7
	12	478.4	112.4	19.0	551.8	135.9	19.7	643.3	162.0	20.1
25	0	475.0			547.5			638.2		
	4	470.2	4.8	1.01	541.6	5.9	1.08	631.0	7.2	1.13
	8	456.9	18.1	3.81	525.0	22.5	4.1	610.9	27.3	4.3
	12	438.0	37.0	7.8	501.2	46.3	8.45	581.8	56.4	8.85
50	0	372.4			414.7			472.8		
	4	371.7	0.7	0.19	413.8	0.9	0.22	471.6	1.2	0.25
	8	369.7	2.7	0.73	411.1	3.6	0.87	468.0	4.8	1.02
	12	366.6	5.8	1.56	406.7	8.0	1.93	462.3	10.5	2.22

TABLE III

Effect of Change of Source Diameter and Temperature on Thickness Distribution for the Deposition of Yttrium

Source to Substrate Distance (cm)	Delta (cm)	Temperature of the Source °K: 2200 Diameter of the Source 1.0" (ΔT)* x10^5 cm/min	2200 Diameter of the Source 1.0" %(ΔT) Change	2200 Diameter of the Source 1.5" (ΔT) x10^5 cm/min	2200 Diameter of the Source 1.5" %(ΔT) Change	2300 Diameter of the Source 1.0" (ΔT) x10^5 cm/min	2300 Diameter of the Source 1.0" %(ΔT) Change	2300 Diameter of the Source 1.5" (ΔT) x10^5 cm/min	2300 Diameter of the Source 1.5" %(ΔT) Change	2400 Diameter of the Source 1.0" (ΔT) x10^5 cm/min	2400 Diameter of the Source 1.0" %(ΔT) Change	2400 Diameter of the Source 1.5" (ΔT) x10^5 cm/min	2400 Diameter of the Source 1.5" %(ΔT) Change
10	0	63.088		139.188		152.193		335.775		338.569		746.964	
	4	47.254	25.1	105.237	24.4	113.995	25.1	253.873	24.5	253.593	25.0	564.766	24.4
	8	23.874	62.4	53.815	61.2	57.592	61.9	129.823	61.4	128.120	62.0	288.803	61.3
	12	10.822	82.8	24.504	82.2	26.107	83.0	59.112	82.5	58.077	83.0	131.500	82.5
15	0	28.289		63.089		68.243		152.194		151.814		338.572	
	4	24.702	12.7	55.210	12.5	59.590	12.7	133.187	12.5	132.563	12.7	296.287	12.5
	8	17.237	39.1	38.691	38.7	41.582	39.1	93.336	38.6	92.504	39.1	207.636	38.6
	12	10.601	62.5	23.874	62.2	25.573	62.5	57.592	62.1	56.891	62.5	128.120	62.1
25	0	10.231		22.945		24.680		55.352		54.904		123.137	
	4	9.728	4.9	21.826	4.87	23.468	4.9	52.652	4.9	52.207	4.9	117.129	4.9
	8	8.426	17.6	18.918	17.6	20.326	17.6	45.637	17.6	45.218	17.6	101.524	17.6
	12	6.769	33.8	15.212	33.8	16.328	33.8	36.698	33.8	36.324	33.8	81.639	33.8
50	0	2.563		5.761		6.182		13.897		13.753		30.916	
	4	2.530	1.29	5.688	1.27	6.103	1.30	13.722	1.26	13.578	1.27	30.526	1.26
	8	2.437	4.92	5.478	4.91	5.878	4.85	13.215	4.80	13.076	4.93	29.400	4.90
	12	2.291	10.60	5.153	10.45	5.527	10.55	12.431	10.55	12.296	11.4	27.655	10.55

* ΔT=Thickness

TABLE IV

Effect of Change of Substrate Material on the Temperature Distribution for the Deposition of Yttrium

Source to Substrate Distance (cm)	Delta (cm)	Temperature of the Source °K: 2200 — Substrate Material: Stainless Steel — Temp.°K	2200 — Stainless Steel — %Temp. Variation	2200 — Copper — Temp.°K	2200 — Copper — %Temp. Variation	2300 — Stainless Steel — Temp.°K	2300 — Stainless Steel — %Temp. Variation	2300 — Copper — Temp.°K	2300 — Copper — %Temp. Variation	2400 — Stainless Steel — Temp.°K	2400 — Stainless Steel — %Temp. Variation	2400 — Copper — Temp.°K	2400 — Copper — %Temp. Variation
10	0	631.1		691.6		718.2		791.1		826.2		915.1	
	4	592.3	6.2	647.1	6.45	673.3	6.25	739.8	6.48	774.4	6.25	855.6	6.5
	8	511.8	18.9	554.7	19.8	579.4	19.4	632.2	20.0	665.0	19.5	730.2	20.2
	12	437.4	30.6	468.7	32.2	490.2	31.8	529.8	33.0	559.3	32.3	609.1	33.5
15	0	530.3		576.0		601.3		657.2		690.6		759.5	
	4	515.4	2.81	558.9	2.98	583.7	2.92	637.1	3.06	670.1	2.97	736.0	3.1
	8	478.7	9.73	516.6	10.3	540.2	10.15	587.3	10.6	618.9	10.4	677.3	10.8
	12	435.7	17.8	466.8	19.0	488.2	17.9	527.5	19.7	556.8	19.3	606.3	20.2
25	0	432.9		463.4		484.7		523.4		552.6		601.4	
	4	428.9	0.93	458.8	1.0	479.8	1.01	517.8	1.07	546.7	1.07	594.7	1.11
	8	418.0	3.45	446.0	3.76	466.2	3.82	502.2	4.05	530.2	4.05	575.8	4.25
	12	402.6	7.0	427.8	7.7	446.9	7.8	479.7	8.36	506.5	8.35	548.5	8.8
50	0	350.9		365.7		378.8		399.5		419.6		447.9	
	4	350.4	0.14	365.1	0.16	378.1	0.18	398.6	0.23	418.7	0.22	446.7	0.27
	8	349.0	0.54	363.2	0.69	376.0	0.74	396.2	0.83	415.9	0.89	443.5	0.99
	12	346.6	1.23	360.3	1.48	372.7	1.61	392.2	1.93	411.5	1.93	438.3	2.14

TABLE V

Time (in seconds) to reach Steady State Temperature for the Deposition of Yttrium

Source Temperature °K	Substrate Thickness (in)	Source to Substrate Distance (cm) 10 Delta (cm)				15 Delta (cm)				25 Delta (cm)				50 Delta (cm)			
		0	4	8	12	0	4	8	12	0	4	8	12	0	4	8	12
2200	0.001	70	70	80	100	70	80	80	100	100	100	110	110	140	140	140	140
	0.005	150	180	240	320	220	230	270	320	320	330	340	370	430	430	430	430
	0.01	260	300	400	540	380	400	460	550	550	560	590	620	690	690	690	690
	0.05	950				1350				2150				3080			
2300	0.001	50	50	60	80	60	60	70	80	80	90	90	90	120	120	130	130
	0.005	120	140	180	260	170	180	210	260	260	270	280	310	400	400	410	410
	0.01	200	230	310	440	290	310	360	440	450	460	490	520	670	670	670	680
	0.05	730				1060				1660				2800			
2400	0.001	40	40	50	70	50	50	60	70	70	70	70	80	110	110	110	110
	0.005	100	110	140	200	130	140	160	200	200	210	220	240	340	340	350	350
	0.01	150	170	240	340	220	230	270	340	350	350	380	410	580	580	590	600
	0.05	530				790				1240				2310			

TABLE VI

Time to Reach Steady State Temperature for the Deposition of Yttria
(seconds)

At the Center of the Substrate (Delta = 0)

Temperature of the Source °K	Thickness of the Substrate in.	Source to Substrate Distance (cm) 10	15	25	50
2,000	0.001	60	70	90	100
	0.005	150	200	270	290
	0.01	250	340	450	460
	0.05	890	1190	1650	1750
2,100	0.001	50	60	80	100
	0.005	120	170	240	300
	0.01	200	280	400	490
	0.05	720	1010	1440	1860
2,200	0.001	40	50	70	90
	0.005	100	130	200	290
	0.01	150	220	330	480
	0.05	540	790	1160	1770
2,300	0.001	40	40	60	80
	0.005	80	100	150	250
	0.01	120	160	250	420
	0.05	390	580	910	1490
2,400	0.001	30	40	50	70
	0.005	60	80	120	200
	0.01	90	120	190	340
	0.05	280	410	670	1170

TABLE VII

Effect of Change of Emittance on Temperatures for the Deposition of Yttrium

Temperature of the Source °K	H (cm)	Delta (cm)	E_1 & E_2=0.35 Temperature °K ①	E_1 & E_2=0.45 Temp. °K ②	Difference between ① & ②	% Difference	E_1 & E_2=0.55 Temp. °k ③	Difference between ① & ③	% Difference	E_1 & E_2=0.65 Temp. °K ④	Difference between ① & ④	% Difference
2,200	25	0	631	650	19	2.92	671	40	5.95	692	61	9.65
		4	592	607	15	2.48	629	37	5.9	648	56	9.47
		8	512	525	13	2.48	541	29	5.35	556	44	8.60
		12	437	447	10	2.24	459	22	4.8	470	33	7.55
		0	433	443	10	2.26	454	21	4.65	465	32	7.4
		4	429	438	9	2.06	449	20	4.45	460	31	7.24
		8	418	427	9	2.10	437	19	4.35	447	29	6.45
		12	403	411	8	1 95	420	17	4.05	429	26	6.45
	50	0	351	356	5	1.4	361	10	2.77	367	16	4.56
		4	350	355	5	1.41	360	10	2.78	366	16	4.56
		8	349	353	4	1.13	359	10	2.78	364	13	3.72
		12	347	351	4	1.14	356	9	2.52	361	14	4.04
2,400	10	0	826	824	2	0.24	828	2	0.24	835	9	1.08
		4	774	772	2	0.26	775	1	0.13	781	7	0.91
		8	665	662	3	0.45	663	2	0.3	668	3	0.45
		12	559	556	3	0.54	556	3	0.54	560	1	0.18
	25	0	553	549	4	0.73	550	3	0.55	553	0'	0
		4	547	543	4	0.74	544	3	0.55	547	0	0
		8	530	527	3	0.57	527	3	0.57	530	0	0
		12	506	503	3	0.6	503	3	0.60	506	0	0
	50	0	420	417	3	0.72	416	4	0.96	418	2	0.48
		4	419	416	3	0.72	416	4	0.96	417	2	0.48
		8	416	413	3	0.73	413	3	0.73	414	2	0.48
		12	412	409	3	0.73	408	4	0.98	410	2	0.49

TABLE VIII

Effect of Change of Emittance on Temperatures for the Deposition of Yttria

Temperature of the source °K	H (cm)	Delta (cm)	E_2=0.35 E_4=0.60 Temperature °K (1)	E_2=0.35 E_4=0.8 Temp. °K (2)	Difference between (1) & (2)	% Difference	E_2=0.35 E_4=0.9 Temp. °K (3)	Difference between (1) & (3)	%Difference	E_2=0.65 E_4=0.90 Temp. °K (4)	Difference between (1) & (4)	% Difference
2,200	10	0	708	693	15	2.12	688	20	2.82	744	36	5.1
		4	663	649	14	2.12	643	20	3.02	696	33	5.0
		8	569	556	13	2.29	551	18	3.16	595	26	4.6
		12	481	470	11	2.29	466	15	3.12	500	19	3.94
	25	0	475	465	10	2.1	461	14	2.94	494	19	4.0
		4	470	460	10	2.12	456	14	2.98	489	19	4.05
		8	457	447	10	2.18	444	13	2.84	475	18	3.94
		12	438	429	9	2.05	426	12	2.74	454	16	3.66
	50	0	372	366	6	1.61	364	8	2.15	382	10	2.69
		4	372	366	6	1.61	364	8	2.15	382	10	2.69
		8	370	364	6	1.62	362	8	2.16	380	10	2.7
		12	367	361	6	1.63	359	8	2.18	376	9	2.45
2,400	10	0	969	935	34	3.52	921	48	4.8	955	14	1.45
		4	906	874	32	3.52	861	45	4.95	892	14	1.55
		8	775	746	29	3.74	734	41	5.3	761	14	1.81
		12	646	622	24	3.71	612	34	5.25	633	13	2.02
	25	0	638	614	24	3.76	604	34	5.35	625	13	2.04
		4	631	607	24	3.8	597	34	5.4	618	13	2.06
		8	611	588	23	3.76	578	33	5.4	598	13	2.12
		12	582	560	22	3.78	551	31	5.3	570	12	2.06
	50	0	473	456	17	3.6	449	24	5.07	463	10	2.12
		4	472	455	17	3.6	448	24	5.08	462	10	2.12
		8	468	452	16	3.42	445	23	4.9	458	10	2.14
		12	462	446	16	3.46	440	22	4.75	453	9	1.95

TABLE IX

Effect of Change of Substrate Emittance on Temperature Distribution for the Deposition of Yttrium

Source to Substrate Distance (cm)	Delta (cm)	Temperature of the Source °K: 2200 Buffed Substrate Temp.°K	2200 Rolled Substrate Temp.°K	2200 Difference	2200 % Difference	2300 Buffed Substrate Temp.°K	2300 Rolled Substrate Temp°K	2300 Difference	2300 % Difference	2400 Buffed Substrate Temp.°K	2400 Rolled Substrate Temp.°K	2400 Difference	2400 % Difference
10	0	631.1	584.6	46.5	7.35	718.1	668.6	49.5	6.9	826.2	774.8	51.4	6.2
	4	592.3	547.7	44.6	7.55	673.3	625.2	48.1	7.15	774.4	723.7	50.7	6.55
	8	511.8	472.7	39.1	7.65	579.4	535.6	43.8	7.55	665.0	617.2	47.8	7.2
	12	437.4	406.4	31.0	7.1	490.2	453.2	37.0	7.55	559.3	516.8	42.5	7.6
15	0	530.3	489.8	40.5	7.65	601.2	556.2	45.0	7.5	690.6	641.9	48.7	7.05
	4	515.4	476.1	39.3	7.62	583.7	539.6	44.1	7.55	670.1	622.1	48.0	7.15
	8	478.7	442.8	35.9	7.52	540.2	499.0	41.2	7.6	618.9	573.0	45.9	7.4
	12	435.7	404.9	30.8	7.05	488.2	451.3	36.9	7.55	556.8	514.5	42.3	7.6
25	0	432.9	402.4	30.5	7.05	484.7	448.2	36.5	7.55	552.6	510.5	42.1	7.65
	4	428.9	399.0	29.9	7.00	479.8	443.8	36.0	7.5	546.7	505.0	41.7	7.65
	8	418.0	389.7	28.3	6.8	466.2	431.7	34.5	7.4	530.2	489.8	40.4	7.6
	12	402.6	376.7	25.9	6.45	446.9	414.6	32.3	7.25	506.5	468.0	38.5	7.6
50	0	350.9	335.6	15.3	4.35	378.8	357.3	21.5	5.7	419.6	391.1	28.5	6.8
	4	350.4	335.2	15.2	4.34	378.1	356.7	21.4	5.65	418.7	390.3	28.4	6.8
	8	349.0	334.1	14.9	4.27	376.0	355.1	20.9	5.55	415.9	388.0	27.9	6.7
	12	346.6	332.4	14.2	4.1	372.7	352.5	20.2	5.4	411.5	384.2	27.3	6.64

TABLE X

Effect of Change of Emittance of the Substrate Surroundings on the Temperature Calculations for the Deposition of Yttrium

Temperature (°K) at the center of the substrate (δ=0)

Temp. of the source °K	H (cm)	Emittance of the Substrate Surroundings					
		0	0.1	0.3	0.5	0.7	1.0
2200	10	624	624	626	627	629	631
	15	517	51[illegible]	521	524	526	530
	25	407	410	415	420	426	433
	50	292	300	313	325	336	351
2300	10	713	714	715	716	717	718
	15	592	593	595	597	599	601
	25	467	469	472	476	480	485
	50	336	341	351	359	368	379
2400	10	823	823	824	825	825	826
	15	685	685	687	688	689	691
	25	541	542	545	547	549	553
	50	391	394	400	406	412	420

TABLE XI

Relative Contributions of Heat Sources for the Deposition of Yttrium

Temperature of the Source °K	Delta (cm)	Source to Substrate Distance (cm) 10		15		25		50	
		Heat due to Radiation $x10^3$cal/sec	Heat due to Condensation $x10^3$ cal/sec	Heat due to Radiation $x10^3$ cal/sec	Heat due to Condensation $x10^3$cal/sec	Heat due to Radiation $x10^3$cal/sec	Heat due to Condensation $x10^3$ cal/sec	Heat due to Radiation $x10^3$cal/sec	Heat due to Condensation $x10^3$cal/sec
2100°K	0	51.28	21.71	22.99	9.89	8.32	3.56	2.08	0.89
	4	38.41	16.30	20.08	8.55	7.91	3.38	2.06	0.88
	8	19.40	8.27	14.01	5.98	6.85	2.93	1.98	0.85
	12	8.80	3.76	8.62	3.69	5.50	2.36	1.86	0.80
2200°K	0	61.76	57.57	27.70	25.99	10.02	9.46	2.51	2.38
	4	46.26	43.23	24.18	22.71	9.52	8.99	2.48	2.35
	8	23.37	21.96	16.88	15.89	8.25	7.79	2.39	2.26
	12	10.59	10.00	10.38	9.80	6.63	6.27	2.24	2.13
2300°K	0	73.78	138.74	33.08	62.71	11.97	22.85	3.00	5.76
	4	55.27	104.24	28.89	54.82	11.38	21.73	2.96	5.69
	8	27.92	53.00	20.16	38.36	9.85	18.84	2.85	5.48
	12	12.66	24.16	12.40	23.67	7.92	15.15	2.68	5.15
2400°K	0	87.48	307.76	39.22	139.36	14.19	50.86	3.55	12.85
	4	65.52	231.40	34.25	121.86	13.49	48.38	3.51	12.68
	8	33.10	117.81	23.90	85.33	11.68	41.95	3.38	12.22
	12	15.01	53.78	14.70	52.69	9.39	33.75	3.18	11.49

TABLE XII

Relative Contributions of Heat Sources for the Deposition of Yttria

Temperature of Source °K	Delta (cm)	Source to Substrate Distance (cm) 10			15			25			50		
		Heat due to radiation	Heat due to condensation	Heat due to reaction	Heat due to radiation	Heat due to condensation	Heat due to reaction	Heat due to radiation	Heat due to condensation	Heat due to reaction	Heat due to radiation	Heat due to condensation	Heat due to reaction
		x 10^3 cal/sec											
2,000	0	72.32	7.31	15.26	32.43	3.30	6.85	11.73	1.20	2.48	2.94	0.30	0.62
	4	54.17	5.49	11.43	28.32	2.88	5.98	11.15	1.14	2.36	2.90	0.30	0.61
	8	27.37	2.78	5.78	19.76	2.01	4.17	9.66	0.99	2.04	2.79	0.29	0.59
	12	12.41	1.27	2.62	12.15	1.24	2.57	7.76	0.79	1.65	2.63	0.27	0.56
2,100	0	87.9	21.63	45.11	39.42	9.76	20.24	14.25	3.55	7.33	3.57	0.89	1.84
	4	65.84	16.25	33.80	34.42	8.53	17.68	13.55	3.38	6.97	3.53	0.88	1.81
	8	33.26	8.25	17.09	24.02	5.97	12.34	11.74	2.93	6.03	3.40	0 85	1.75
	12	15.08	3.76	7.75	14.77	3.68	7.59	9.43	2.35	4.85	3.19	0.80	1.64
2,200	0	105.88	57.26	119.47	47.48	25.88	53.63	17.17	9.43	19.41	4.30	2.38	4.87
	4	79.31	43.03	89.52	41.46	22.63	46.83	16.33	8.97	18.46	4.25	2.35	4.80
	8	40.07	21.88	45.26	28.93	15.83	32.69	14.14	7.78	15.99	4.09	2.26	4.63
	12	18.16	9.97	20.53	17.79	9.77	20.11	11.36	6.25	12.85	3.85	2.13	4.35
2,300	0	126.49	137.64	287.94	56.72	62.34	129.26	20.51	22.76	46.80	5.14	5.75	11.74
	4	94.74	103.50	215.76	49.52	54.52	112.89	19.50	21.65	44.51	5.07	5.68	11.59
	8	47.86	52.71	109.11	34.56	38.18	78.81	16.89	18.77	38.55	4.89	5.47	11.16
	12	21.70	24.06	49.51	21.25	23.58	48.50	13.57	15.10	30.98	4.59	5.14	10.49
2,400	0	149.96	304.37	639.88	67.24	138.21	287.28	24.32	50.58	104.04	6.09	12.80	26.10
	4	112.32	229.11	479.50	58.72	120.91	250.90	23.12	48.12	98.94	6.01	12.64	25.76
	8	56.75	116.91	242.50	40.97	84.75	175.17	20.03	41.73	85.70	5.79	12.18	24.81
	12	25.72	53.47	110.04	25.20	52.39	107.80	16.09	33.59	68.87	5.45	11.46	23.33

TABLE XIII

Data Used in These Computations

Symbol	Parameter	Value	Reference
M	Molecular weight of yttrium	88.905	13
ρ	Density of yttrium	4.45 g/cm^3	13
σ	Stefan-Boltzmann constant	1.356×10^{-12} $cal/°K^4$-sec	14
ε_l or ε_d	Total hemispherical emmittance of Y assumed to be the same as spectral emittance of yttrium (λ=0.65μ)	0.35	15
ε_d	Total hemispherical emittance of Y_2O_3 assumed to be the same as spectral emittance of oxidized yttrium	0.60	15
ε_s	Total hemispherical emittance of copper	$\{0.01+(T-273)x9.09x10^{-5}\}$	15
ε_s	Total hemispherical emittance of buffed stainless steel	$(0.066+0.267xTx10^{-3})$	16
ε_s	Total hemispherical emittance of rolled stainless steel	$(0.4025 + 10^{-4} \times T)$	16
	Specific heat of copper	$(0.085 + 0.236 \times 10^{-4}xT)$	17
	Specific heat of stainless steel	$(0.120+0.300x10^{-4}xT)$ cal/g.	16
	Specific heat of yttrium	$(5.59+1.9x10^{-3}xT+0.29x10^{5}/T^2)$ cal/deg-mole.	17
	Specific heat of yttria	$(29.60+1.20x10^{-3}xT-4.78x10^{5}/T^2)$ cal/deg-mole	17
	Heat of reaction of $2\ Y_{(s)} + 3/2\ O_{2(g)} \rightarrow Y_2O_{3(s)}$	$-\Delta H°_{298}$=455.4 $\pm$ 1.5 K cal/mole.	18
	Density of copper	8.96 g/cm^3	13
	Denisty of stainless steel	7.90 g/cm^3	19

LIST OF FIGURES

Security Classification

DOCUMENT CONTROL DATA - R & D

(Security classification of title, body of abstract and indexing annotation must be entered when the overall report is classified)

1 ORIGINATING ACTIVITY (Corporate author)
School of Engineering & Applied Science
University of California at Los Angeles
Los Angeles, California 90024

2a. REPORT SECURITY CLASSIFICATION
Unclassified

2b. GROUP
---

3 REPORT TITLE
I. New Methods of Synthesis of Materials

II. The Properties of Rare Earth Metals and Alloys

4 DESCRIPTIVE NOTES (Type of report and inclusive dates)
Semi-Annual Technical Report

5 AUTHOR(S) (First name, middle initial, last name)
I. R. F. Bunshah
II. D. L. Douglass

6 REPORT DATE	7a. TOTAL NO. OF PAGES	7b. NO. OF REFS
March 1, 1971	68 pages	30 references

8a. CONTRACT OR GRANT NO	9a. ORIGINATOR'S REPORT NUMBER(S)
AO #1643	UCLA ENG. 7112
b. PROJECT NO	
c.	9b. OTHER REPORT NO(S) (Any other numbers that may be assigned this report)
d.	

10 DISTRIBUTION STATEMENT
Distribution of this document is unlimited

11 SUPPLEMENTARY NOTES	12. SPONSORING MILITARY ACTIVITY
	Advanced Research Projects Agency, Department of Defense

13 ABSTRACT

Two major areas of effort are encompassed:

I. New Techniques for the Synthesis of Metals and Alloys.

The High Rate Physical Vapor Deposition (HRPVD) process is to be used for the following:

1. Preparation and characterization of Ni and Ni-20Cr alloy sheet
2. Synthesis of compounds Y_2O_3, TiC, Si_3N_4 by reactive evaporation and their characterization
3. Dispersion strengthened alloys, Ni-20Cr-Y_2O_3, Ni20Cr-TiC and Ti-Y_2O_3

This report describes the HRPVD apparatus. Models for calculation of temperature and thickness distribution of the deposit are given.

II. The Properties of Rare Earth Metals and Alloys.

Small amounts of certain rare-earth elements in Nickel-base alloys are known to markedly reduce the rate of oxidation at high temperatures and confer mechanical stability on the scales found. This program is directed at obtaining an understanding of the mechanisms and to characterize the oxidation behavior of Ni-20Cr containing, Gd, La and Y and alloys based on composition Ni_3Al.

DD FORM 1 NOV 68 1473

Security Classification

14 KEY WORDS	LINK A		LINK B		LINK C	
	ROLE	WT	ROLE	WT	ROLE	WT
Condensation						
Deposit						
Deposition Temperature						
Evaporation						
Evaporation apparatus						
Gadolinium						
High Rate Physical Vapor Deposition Process						
Lanthanum						
Nichrome						
Nickel						
Oxidation						
Oxidation mechanism						
Rare-earth additions						
Scale formation						
Silicon nitride-Si_3N_4						
Substrate						
Thickness distribution						
Titanium carbide						
Yttria-Y_2O_3						
Yttrium						

AD-722 088

ERRATA SHEET

TO: Distribution

Semi-Annual Technical Report No. 1
"New Techniques for Synthesis of Metals and Alloys"
R. F. Bunshah UCLA Engr. #7112, March 1971
on ARPA Grant No. DAHC 15-70 G 15

Please correct the following errors in the report:

	Reads	Should Read
pg. 1.4, line 7	R - energy radiated ...	R_s-energy radiated ...
pg. 1.4, eq. 9	$dA_2 F_{dA_2-A_1} t \int^{\infty} \varepsilon_1(\lambda,T_1)$ ...	$dA_2 F_{dA_2-A_1} t \int_0^{\infty} \varepsilon_1(\lambda,T_1)$ ...
pg. 1.6, eq. 14	$_s(T_2)$ = ...	$\varepsilon_s(T_2)$ ...
pg. 1.9, eq. 25	H_ℓ(at 7735°K) = L ρ...	H_ℓ(at 1135°K) = L_sρ ...
pg. 1.9, line 14	1155°K	1155°K = $L_t \rho \delta dA_2$
pg. 1.9, eq. 26	... = 3.83×10^8 ergs	... = $3.83 \times 10^8 dA_2$ ergs
pg. 1.10 line 2	... T_2 = 913°K for Run 41	... T_2 = 887°K for Run 41